# Molecular Insights on the Solvent Effect of Methanol Additive in Glycine Polymorph Selection

by

Srikanth Patala

Submitted to the Department of Materials Science and Engineering
in partial fulfillment of the requirements for the degree of

Master of Science

at the

MASSACHUSETTS INSTITUTE OF TECHNOLOGY
[June 2008]
May 2008

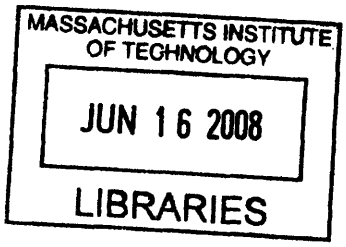






Author .....
Department of Materials Science and Engineering
May 30, 2008

Certified by .....
Bernhardt L. Trout
Associate Professor of Chemical Engineering
Thesis Supervisor

Certified by .....
Samuel M. Allen
POSCO Professor of Physical Metallurgy
Thesis Reader

Accepted by .....
Samuel M. Allen
POSCO Professor of Physical Metallurgy
Chair, Departmental Committee on Graduate Students

# Molecular Insights on the Solvent Effect of Methanol Additive in Glycine Polymorph Selection

by

Srikanth Patala

Submitted to the Department of Materials Science and Engineering
on May 30, 2008, in partial fulfillment of the
requirements for the degree of
Master of Science

## Abstract

In an effort to improve control and design in organic crystallization, the effect of solvent on polymorph selection has gained tremendous interest in recent years. In this thesis, molecular simulation techniques are used to gain insight into the solvent effect on glycine crystallization in water-methanol mixtures. We report the validation of the Optimized Potential for Liquid Simulations (OPLS) force field and parameters with modified Lennard-Jones parameters for hydrogens attached to $\alpha$-carbon in glycine zwitterion. Solution and interface simulations in water and 50% v/v water-methanol solutions reveal the mechanism through which methanol additive results in the crystallization of the least stable $\beta$-glycine polymorph. Free energy calculations through the Umbrella Sampling method show an increased stability of the centrosymmetric dimer structure ($\alpha$-glycine growth unit) in the presence of the methanol additive. Even though the dimer structure is more stable in water-methanol mixtures, a higher fraction of glycine monomers were observed in water-methanol mixtures. It is revealed through thermodynamic arguments that a drastic decrease in solubility results in a higher fraction of glycine monomers in water-methanol mixtures. It was hypothesized in previous studies that the presence of monomer units docking onto the (010) interface of $\alpha$-glycine inhibits further growth due to exposed ammonium groups at the interface. The effect of solvent on crystal growth inhibition is explored by the interface simulations of $\alpha$-glycine in water-methanol mixtures. When the monomer units are docked onto the interface, water is shown to be more effective than methanol in inhibiting crystal growth of (010) interface of $\alpha$-glycine. This study sheds light on the role played by the solvent on glycine polymorph selection in water-methanol solutions.

Thesis Supervisor: Bernhardt L. Trout
Title: Associate Professor of Chemical Engineering

# Acknowledgments

My experience at MIT has been both exciting and challenging to say the least. The most exciting part is getting the opportunity to work on this project under the guidance of my advisor, Prof. Bernhardt L. Trout. I am extremely grateful for his belief in me and also for his constant support and invaluable advice throughout the project.

I owe a great deal to Dr. Gregg Beckham without whom this study would be incomplete. I thank him for teaching me how to use CHARMM and also for many invigorating and creative ideas. I am greatly indebted to Jie Chen for her assistance during many stages of this project, Dr. Naresh for his encouragement and advice throughout, and Bin Pan for his help in solving many technical problems and for his wonderful Chinese tidbits. The Trout Group presented me with a stimulating and fun filled atmosphere and I am very thankful for the opportunity to interact with them. A special thanks to Prof. Samuel Allen, Materials Science Department Chair, who has been very kind and helpful in sharing his invaluable time with me during the course of my stay here.

Any of my experiences at MIT would not have been so compelling without some of the wonderful people that I have gotten to know in the last two years: Srujan, with whom I had many memorable and inspirational moments; Dipanjan and Sukant who endured all my tantrums as roommates and have been a great source of encouragement; Chetan, Ashish and Deep who always had insightful opinions about my professional and personal life. I would also like to thank my parents and family who have given me this great opportunity and always encouraged me to follow my dreams.

Finally, I would like to thank the Singapore MIT Alliance Flagship Research Program and the Department of Materials Science and Engineering for financial support during my studies.

# Contents

# List of Figures

# List of Tables

# Chapter 1

# Introduction

Understanding the control of polymorphism in organic crystals is of paramount importance to pharmaceutical and food industries and others, and is also of theoretical relevance in solid state chemistry and physics. Significant variability in product performance in the chemical and food industry has been attributed to polymorphism, and it continues to pose a challenge to pharmaceutical industries to produce drugs of consistent quality. Polymorphism occurs when a molecule packs in different ways, giving rise to two or more crystal structures. Organic compounds owing to their size and floppiness result in various plausible polymorphs, sometimes with close thermodynamic stability. These polymorphs differ significantly in physical and chemical properties, making polymorphic control in manufacturing absolutely necessary . Differences in solubility between crystal forms of a pharmaceutical can lead to differences in bioavailability in solid dosage, if bioavailability is dissolution limited.

Crystallization from solutions is the most commonly used and critical step in pharmaceutical manufacturing for polymorph selection. Cases with solvent affecting the final polymorphic outcome have been widely reported [2], but the underlying mechanisms still remain unclear. Research on polymorphism is fraught with unique difficulties due to subtlety in polymorphic transformations. Exploring the molecular self-assembly process during the nucleation process has proved very challenging, both experimentally and computationally.

The growth synthon hypothesis [2] tries to establish a link between liquid phase

molecular assemblies and their solid state counterparts in the final crystal, but exceptions to this rule exist. Tailor made additives [5] have been extensively used to manipulate the final crystal outcome by inhibiting growth of certain polymorphs, but their applicability has been found only in limited systems like glycine, alanine etc. The mechanisms through which solvent affects polymorphic selection still remains uncertain and much exciting work is to be done. The solvent selection process is mostly restricted to heuristic experimental screens, and any rational guidelines are extremely desired.

## 1.1 Objectives & Overview

The purpose of this thesis is to gain molecular level perspective into the solvent effect on crystallization through the use of simulation techniques like Molecular Dynamics and Umbrella Sampling [6]. Glycine crystallization in water and water-methanol mixtures is the model system chosen to study these effects. It has been observed that glycine crystallizes in its least stable form when precipitated from water-methanol solutions [4]. This system is investigated to better understand the underlying mechanisms which could lead to rational selection of solvents.

The thesis is organized in six chapters. Chapter 2 discusses the nucleation and growth processes in crystallization from solutions and the relevant literature review of the solvent effect on polymorph selection during these stages.

In Chapter 3, the polymorphism exhibited by glycine and the effect of water and methanol on the final crystal polymorph is discussed in detail. The hypothesis underlying the crystallization of the least stable $\beta$-glycine from water-methanol mixtures, as proposed by Weissbuch et al. [4], is discussed in this chapter.

It is our objective to test this hypothesis and gain molecular level insights into the solvent effect on polymorph selection. For this purpose, molecular level simulations of glycine in solutions and solvent-crystal interfaces were carried out. Chapter 4 discusses the validation of force fields and parameters for glycine polymorphs. In Chapter 5 the results obtained from the solution and interface simulations of glycine

are presented and discussed in the light of the proposed hypothesis [4]. Chapter 6 summarizes the findings with major conclusions and suggestions for future work.

# Chapter 2

# Organic Crystal Polymorphism

## 2.1 Introduction

Polymorphism is the ability of a molecule to 'stack' into different molecular conformations while retaining the same chemical composition [7]. In the pharmaceutical industry, a very large number of pharmaceuticals exhibit the phenomenon of polymorphism. 70% of barbiturates, 60% of sulfonamides and 23% of steroids exist in different polymorphic forms [8]. The existence of polymorphism in the case of antiviral drug Ritonavir has had dramatic commercial effect on pharmaceuticals. The manufacture of Norvir (commercial name for Ritonavir) semi-solid capsules formulation involved the preparation of a hydroalcoholic solution of Ritonavir which, although not saturated with respect to form I was 400% supersaturated with respect to form II. The sudden appearance and dominance of this dramatically less soluble crystal form made the formulation not manufacturable [9]. It was necessary to immediately reformulate Norvir. These factors combined to limit inventory and seriously threatened the supply of this life saving treatment for AIDS. Another classic example is polymorphism exhibited by compound ROY [1]. Six solvent free polymorphs of ROY are shown in Figure 2-1. Glycine, a simple amino acid, can pack itself in three different crystal structures.

Polymorphism and polymorphic transformations of organic systems have been studied extensively since development of X-ray diffraction techniques. Earlier studies

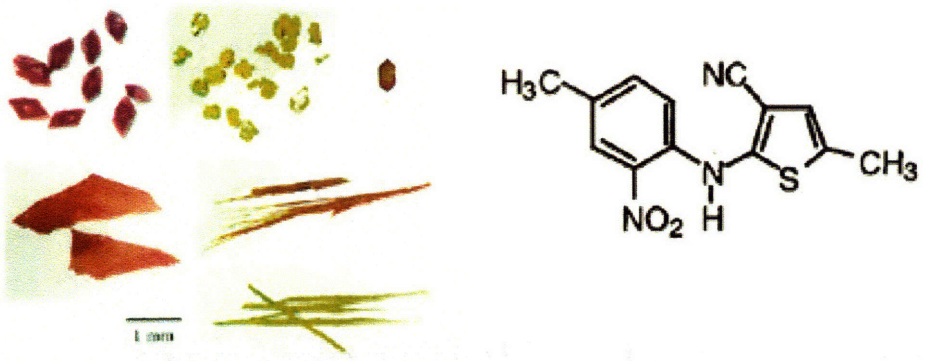


Figure 2-1: Polymorphs of ROY. [1]

mainly focused on characterization of crystal structures of various organic compounds and methods of manufacturing these polymorphs [10]. Recent studies typically examine conditions under which polymorphic transformations occur including humidity, pressure, solvents, additives and other process induced transformations [5, 11–14]. Early computational investigations typically focused on ab initio polymorph prediction of various organic systems [15]. Recent studies on atomistic simulations of solutions and organic crystal interfaces provide molecular level insights into polymorphic selection [16, 17].

Effect of solvents on organic crystal polymorphism has gained importance because the use of solution phases as media for homogenization and crystallization for the subsequent assembly processes are common [2]. Understanding the mechanistic role of solvents in polymorph selection is of great significance. Solvent is an important consideration in solution crystallization, which affects the morphology, size distribution, downstream processing, as well as polymorph of the final product. In pharmaceutical industries, solvent screening is the first and the most important step in polymorph study. Despite this, surprisingly little is known about the molecular self assembly processes that surround the nucleation event and in particular the link between solution speciation, molecular aggregation and the nature of intermolecular interactions in the resulting crystal. This gap in understanding is particularly evident in systems which exhibit crystal polymorphism, when small changes in solvent choice

and crystallization conditions can yield a new crystal structure. Several studies, both experimental and computational, have been conducted to gain insights into the effect of solvents on crystallization [16–18]. The process of crystallization from solution can be divided into two stages: nucleation event to form an embryo, and the growth of the embryo into a crystal. Solvent plays a major role during both these stages and hence influencing the final crystal structure. In the following sections the relevant literature on the solvent effect during nucleation and growth stages is reviewed.

## 2.2 Nucleation Controlled Polymorph Selection

### 2.2.1 Nucleation Theory

The process of nucleation has been the subject of almost continuous study over the past 150 years [19]. The first notable observations were made by Ostwald concerning the effect of sample volume, seeding and metastable states. Ostwald Rule of stages [20] summarizes the complex interplay between thermodynamic and kinetic factors in nucleation. Ostwald indicates that in a polymorphic system the crystallization process starts with the appearance of the least stable of the known forms. This is the first indication that the polymorphic outcome during crystallization is not a fixed parameter rather it will be determined by the underlying kinetic processes reflected by the crystallization pathway. Paracetamol, for example, crystallized from acetone solution will always yield crystals of the stable monoclinic form I whereas crystallization from the melt will always produce the orthorhombic metastable layer structure, form II [21].

Classical nucleation theory originated in the 1930s and is largely attributed to work by Becker, Döring and Volmer [22, 23]. The kinetic formulism was further developed by Volmer [24]. The basic idea is that thermal fluctuations give rise to the appearance of small nuclei of a second phase and occasionally produce a long chain of favorable energetic fluctuations, thereby creating a nucleus exceeding the critical size [25]. Although this second phase has favorable lower free energy, there is a free energy

penalty associated with the creation of an interface. Hence nucleation is an activated process in which the transition state is associated with an assembly of molecules held together by intermolecular interactions and interface structure. The free energy $\Delta$G, of second phase is the sum of a negative volume term and a positive surface term. For a spherical nucleus, $\Delta$G is given by

$$\Delta G = -\frac{4}{3}\pi R^3 \Delta G_v + 4\pi R^2 \gamma \tag{2.1}$$

where, $R$ = radius of the nucleus, $\Delta G_v$ = bulk free energy difference per unit volume between the first and second phases, and $\gamma$ = surface free energy of the second phase per unit area. The maximum of the free energy in 2.1 corresponds to the critical size of the nucleus $R_{critical}$, given by

$$R_{critical} = -\frac{2\gamma}{\Delta G_v} \tag{2.2}$$

Combining equations 2.1 and 2.2 produces an expression for the maximum free energy barrier of nucleation, $\Delta G_{critical}$,

$$\Delta G_{critical} = \frac{4}{3}\pi \gamma R^2{}_{critical} \tag{2.3}$$

From 2.3, the rate of nucleation $J$, can be expressed using transition state theory,

$$J = A \exp\left(\frac{-\Delta G_{critical}}{kT}\right) \tag{2.4}$$

where, $A$ = frequency factor, $k$ = Boltzmann Constant, $T$ = temperature.

However, several fundamental limitations exist in classical nucleation theory. The first is that the critical nucleus is treated as a bulk phase, and the surface is modeled as an infinite plane. These assumptions seemingly do not hold if the critical nucleus is on the order of a few nanometers. In addition, classical nucleation theory does not provide information regarding the formation of the critical nucleus. A nonclassical theory of nucleation has been developed by Oxtoby et al. to overcome the limitations

posed in classical nucleation theory [26, 27]. Instead of treating the critical nucleus as bulk material, the free energy of the second phase is quantified via density functional theory. These types of non-classical nucleation theories serve to overcome, albeit qualitatively, a number of shortcomings of classical nucleation theory. However, these models still do not accurately capture the process of nucleation [27].

The kinetic theories were developed to explain macroscopic phenomena at time when the available experimental techniques were restricted to a resolution of 1.0 mm at best. The advent of modern techniques and methodologies, including atomic probe microscopes, neutron diffraction and scattering and molecular modeling, have led us routinely to expect resolution and visualization down to 0.1 nm, an advance which has only just begun to be reflected in experimental and theoretical studies [28, 29] of the nucleation process. There is growing evidence that nucleation from solution is itself a two-step process. The first step involves the formation of a liquid like cluster of solute molecules, while the second involves the reorganization of such a cluster into an ordered crystalline structure [30–32]. ten Wolde and Frenkel considered solute-solute interactions given by a modified Lennard-Jones potential and proposed the presence of a metastable fluid-fluid critical point close to which the free energy barrier for crystal nucleation is strongly reduced and the nucleation rate increases by many orders of magnitude [30]. Anwar and Boateng showed by molecular simulations that crystallization in highly supersaturated systems involves liquid-liquid phase separation followed by nucleation of the solute phase [31]. By using molecular dynamics to study the nucleation of AgBr in water, Shore et al. have provided further evidence to the conjecture that nucleation of crystals from solution may be a two-stage process [32]. They have further suggested that disordered clusters are actually the stable state until the cluster size becomes rather large. Using small-angle X-ray scattering, Chattopadhyay et al. have directly studied the nucleation of the amino acid glycine from its aqueous supersaturated solution [33]. Their results are consistent with a two-step nucleation process.

Even with the advent of these techniques, determination of the structure of the critical nucleus has proven to be a daunting task in simple single component sys-

tems like water [34], nitrogen [35] and carbondioxide [36]. This problem still remains unsolved for systems involving two or more components, for e.g. a solution. Even though the structure of critical nucleus remains unresolved, an important result deduced through the use of these advanced techniques is the Growth Synthon hypothesis [2] that connects the solvent-solute interactions to the crystal structures obtained. This is explained in the following section.

### 2.2.2 Growth Synthon Hypothesis

Crystal engineering has spawned the notion of the structural synthon and growth synthons. The structural synthon refers to the hydrogen bond structure of the building blocks in the crystal packing motifs and have been derived from the vast amount of crystal structure data available. The growth synthons (or 'growth units') refer to the conformations exhibited by the solute molecules in the solutions. The understanding of the link between the growth unit and the structural synthon then becomes the basic structural problem for nucleation theory. The growth synthon hypothesis suggests that the most stable growth synthon has the highest probability to pack into crystal as the structural synthon which can be seen using XRD.

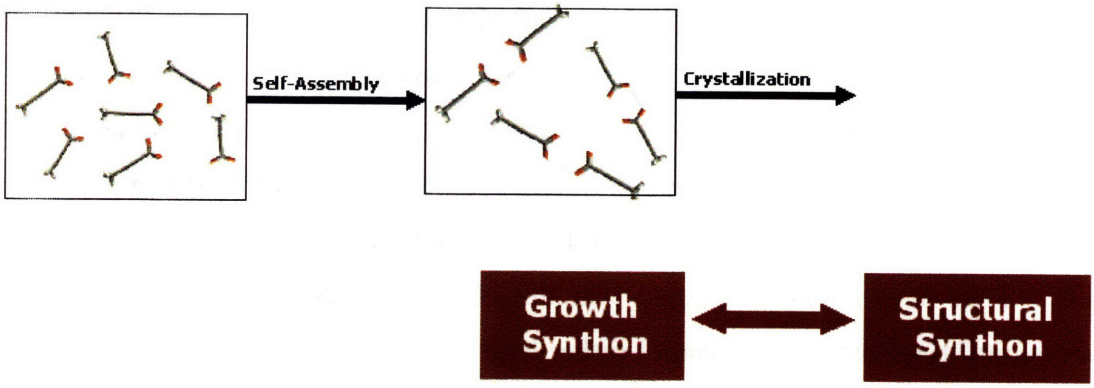


Figure 2-2: The link between self-assembly in solution and its crystal structure.

The growth synthon hypothesis was successfully used to explain the polymorphic behavior of tetrolic acid. Davey et al. [37] detected the presence of carboxylic dimers formed by two tetrolic acid molecules in chloroform using FTIR, which is consistent

with the dimer structure (structural synthon) present in the crystal obtained from chloroform solution. They also found that, when ethanol used as the solvent, no dimer structure can be seen in solution, which is consistent with the fact that no dimer structure is present in the crystal obtained from ethanol. The relation between the growth and structural synthon for tetrolic acid is shown in Figure 2-2.

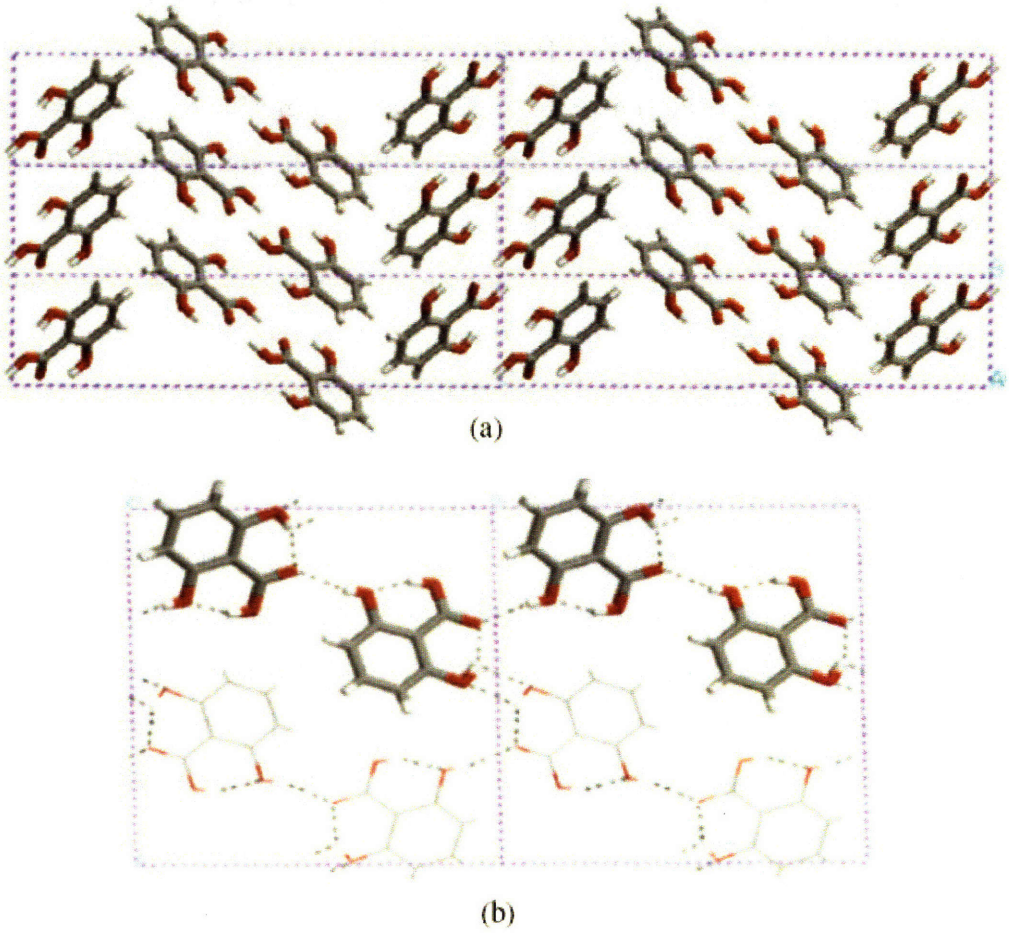


Figure 2-3: Two polymorphic forms of 2,6-dihydroxybenzoic acid: (*a*) the metastable form 1 dimer structure, and (*b*) the stable form 2 catemeric structure [2].

A Similar trend was observed in the case of 2,6-dihydroxybenzoic acid. The acid exists in only two known polymorphic forms: form I is a metastable monoclinic form based on centrosymmetric carboxyl dimers [38] while the stable form II is noncentric based on a catemer motif which utilizes a carbonyl-hydroxy interaction [39]. Figure 2-3 shows the structural elements of these two structures. In this case it was found that

in quiescent solutions the metastable dimer structure nucleated preferentially from toluene, whereas in chloroform direct nucleation to the stable form was possible. A combination of solubility data, UV/vis spectroscopy and calculation of solvation enthalpies all pointed to the preferential assembly of dimers in toluene solutions and catemers in chloroform, yielding again a clear link between the assembly process in solution and the nucleation event [40]. A further example is the case of glycine. From aqueous solutions, at the isoelectric pH of 6.1, glycine crystallizes in its metastable centrosymmetric $\alpha$ form. The consistent appearance of $\alpha$-glycine has been explained by the existence of centrosymmetric zwitterionic dimers in aqueous solution which naturally pack to yield the $\alpha$ structure [41].

However, limitations to the growth synthon hypothesis still exist. For example mandelic acid crystallizes in a dimer based form from its racemic solution, although no dimer based growth synthon can be detected in solution [42]. Even there exists no direct data that relate to the structure of the molecular clusters that are smaller than critical size. The growth synthon hypothesis provides some evidence that molecular assembly in the liquid phase can mirror the packing of the potential polymorphs in a system. The nature of the solvent-solute interactions, however, can play a significant role in determining the viability of these clusters and hence direct the structural outcome of the crystallization. The understanding of the link between the growth unit and the structural synthon remains the basic problem for nucleation theory and much exciting work remains to be done.

## 2.3 Growth Controlled Polymorph Selection

### 2.3.1 Crystal Growth in Solutions

It was very well known that solvent affects the crystal shapes, i.e., the ratio of growth rates of their various faces [17]. The effects of solvent on crystal growth have been extensively studied for over a century. Historically it was probably the work of Wells [43] which first drew the attention to the importance of solvent in determining growth

morphology. Using resorcinol as an example he illustrated the significance of a solvent specific interaction with different crystal faces. According to Wells, the faces terminating in hydroxyl groups of resorcinol are blocked by water molecules. This leads to preferential development of these faces during the formation of resorcinol crystals. The nonpolar solvent benzene does not affect this selective adsorption. The crystal grows symmetrically in opposite directions. Other studies followed Well's work and in particular the works of Watson [44] and Kleber and Raidt [45] are worth noting. These works were the first to link growth behavior to solution chemistry.

In general, the crystal growth kinetics from solutions is governed by two factors relating to the nature of the growing interface [18]. One is related to the degree of molecular roughness as determined by the energetics of step creation at the surface and the other is concerned with the stereo and thermo chemical nature of adsorption of solvent on the surface [46].

***Surface Roughness:*** In the statistical mechanics description of the interface between a solid and fluid phase the roughness is quantified in terms of the $\alpha$ factor [46]. The $\alpha$ factor defines the enthalpy change which takes place when a flat interface is roughened [47]. The value of $\alpha$ can be related to the expected growth mechanism of a face. According to the surface roughness theory if $\alpha \leq 3$, the interface is rough, and the growth is linearly dependent on the supersaturation. If $\alpha$ is greater than 4, the interface is smooth, and the growth occurs at the steps generated by defects of surface nucleation.

***Surface Adsorption:*** In terms of the crystal growth process it is important to consider the nature of the interaction between individual solvent and solute molecules since incorporation of a solute molecule in a growth site requires desorption of solvent molecules. For certain combinations of solvent and solute interfaces it is conceivable that there could be strong adsorption of solvent in the growth sites hence reducing the growth rate of that interface. No general formalism exists to describe the relationship between adsorption and growth rate. Each example has to be considered in turn due to the specificity of molecular

packing in the solid phase [18]. When the solvent-solute intermolecular interactions are strong the solute molecules are solvated and the growing surfaces of the crystals are covered by solvation layers which must be removed prior to the deposition of additional layers. The degree of solvation which is determined by the structure of the surface layer may vary from one face to another.

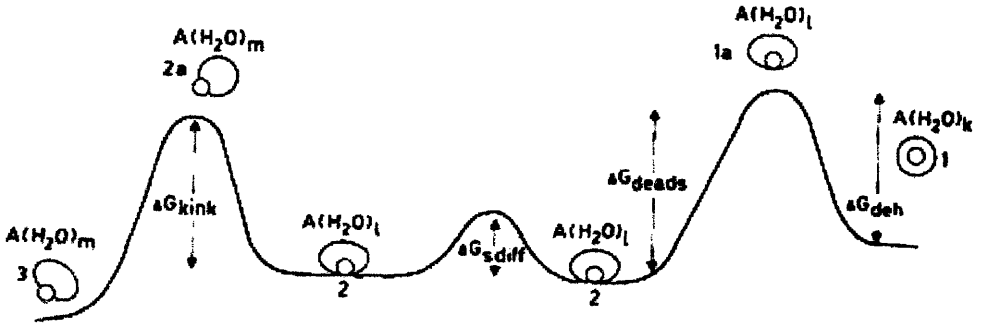


Figure 2-4: An illustration of various processes involved in the crystal growth process from aqueous solutions [3].

The above two factors are qualitative indications of the growth mechanisms and solvent effects on growth interfaces. A more general formulism for crystal growth from solutions is developed by Bennema [3] by adapting the Burton, Cabrera and Frank surface diffusion model [48]. According to this theory, the first step in crystallization from solutions is desolvation of the crystallizing solute molecules and the surface sites, and then the entrance of the solute molecule into the solvation layer of the faces. This is followed by surface diffusion until a step is reached permitting incorporation into the crystal lattice at a kink site. The activation free energies associated with these respective steps are $\Delta G_{deh}$ (dehydration activation free energy for entering the surface layer), $\Delta G_{sdiff}$ (activation free energy for making a diffusion jump from one equilibrium position to a neighboring one in the surface layer) and $\Delta G_{kink}$ (activation free dehydration energy for the entry of growth units into kinks from the surface layer). Figure 2-4 illustrates the various processes involved in the crystal growth process from aqueous solutions.

It is qualitatively important to understand the free energy barriers that dominate

the growth process. $\Delta G_{deh}$ and $\Delta G_{sdiff}$ are both dependent on the interactions between the solute and solvent molecules. It is generally true that $\Delta G_{sdiff}$ is much less than $\Delta G_{deh}$ for crystal growth from solutions. All three free energies are different on different faces. For growth from the vapor phase $\Delta G_{deh} = 0$ and the rate determining step is $\Delta G_{kink}$. It is also important to note that for layer growth mechanism (where the creation of kink is not necessary), $\Delta G_{deh}$ determines the rate of crystal growth. Therefore, for growth from the solution, strong interactions between solute and solvent at specific crystal faces may lead to $\Delta G_{deh} >> \Delta G_{kink}$, and thus the desolvation of specific crystal faces becomes the rate determining step.

### 2.3.2 Crystal Growth in Polar Organic Crystals (*"Relay Type" Growth Mechanism*)

A very interesting case with an entirely different approach towards crystal growth from solutions is observed in the growth of polar organic crystals like $\gamma$-glycine and (R-S)alanine. These two crystals have similar packing features and only the growth of $\gamma$-glycine is discussed here. $\gamma$-glycine in solutions has a flat $(00\bar{1})$ face perpendicular to the polar c-axis at one end and capped faces at the opposite end as shown in Figure 2-5 [49]. According to crystal growth and etching experiments [50, 51] the $CO_2^-$ groups are exposed at the $(00\bar{1})$ face, the "flat -c end", while the $NH_3^+$ amino groups are exposed at the $+$c capped end [50, 51]. Various experiments involving the comparison of the relative rates of growth and dissolution of the crystals of (R-S)alanine and $\gamma$-form of glycine indicate that in aqueous solutions the $-c$ carboxylate end of the crystals grow and dissolve faster than the $+c$ amino end.

Inspection of the packing arrangement of $\gamma$-glycine Figure 2-6 reveals that (001) carboxylate faces comprise regular pockets on a molecular level and can be regarded as corrugated in two dimensions. The binding of water in these pockets can be qualitatively explained by looking at the water-glycine interactions in the pocket. The water molecules inside the pocket can essentially take two different orientations; one orientation comprises of O—H$\cdots$O hydrogen bond and two O–O lone-pair-lone-

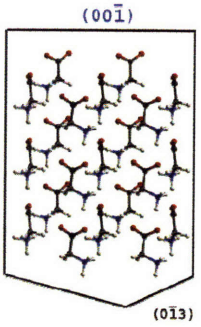


Figure 2-5: Packing arrangement of $\gamma$-glycine delineated by crystal faces, as viewed down the b-axis. The capped faces at the $+c$ end of the polar axis expose $NH_3{}^+$ groups at their surface the opposite faces expose $CO_2{}^-$ groups.

pair repulsions and the other two O—H$\cdots$O bonds and one O–O lone-pair-lone-pair repulsion. Consequently introduction of water yields repulsive or at best weakly attractive interactions. The pocket will therefore be unhydrated or slightly hydrated and relatively easily accessible to approaching solute molecules as shown in Figure 2-6. In contrast, the water molecule may be strongly bound to the outermost layer of $CO_2{}^-$ groups via O—H$\cdots$O (carboxylate) hydrogen bonds.[1] As glycine molecules are incorporated into adjoining pockets, the $CO_2{}^-$ groups of newly added substrate molecules will expel the water bound on the outermost surface, thereby generating new unsolvated pocket on the crystal surface. This relay process of solvent water binding and expulsion helps growth and dissolution by both desolvating the surface and perpetuating the natural corrugation of the surface, at a molecular level (Figure 2-6).

A general relay type mechanism is depicted in Figure 2-7. The difference between two types of sites (A & B) is emphasized by assuming a corrugated surface such that the A-type site is a cavity and the B-type site is on the outside upper surface of the cavity. Figure 2-7($a$) shows the B-type sites blocked by solvent S and the A-type sites unsolvated. Thus solute molecules can easily fit into A-type sites. But once docked into position (Figure 2-7($b$)) the roles of the A and B-type sites are essentially

[1]The water molecules bound to the outermost layer of groups via O-H–O hydrogen bonds provide additional stabilization energy to the (001)surface layer which has a low molecular density with all molecular dipoles pointing approximately in the same direction.

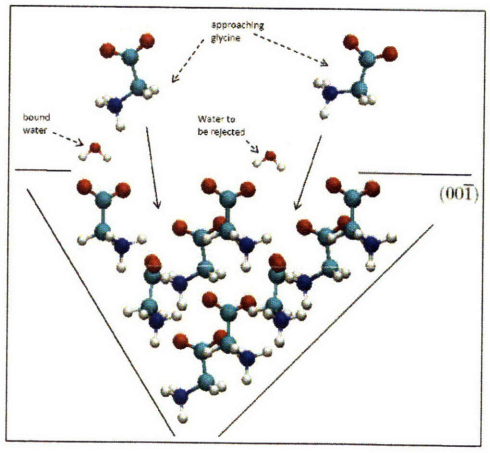


Figure 2-6: Packing arrangement of $\gamma$-glycine as viewed down the b-axis, depicting the relay mechanism at (00$\bar{1}$) interface. The bound water molecules are ejected from the pockets as glycine from solution approach the interface.

reversed and the solvent molecules which originally were bound to B-type sites would be repelled since they now occupy A-type sites. This cyclic process can lead to fast growth. In such a situation described here, where desolvation is rate limiting, it is implicitly indicated that the free energy of incorporation of a solute molecule helps to displace bound solvent.

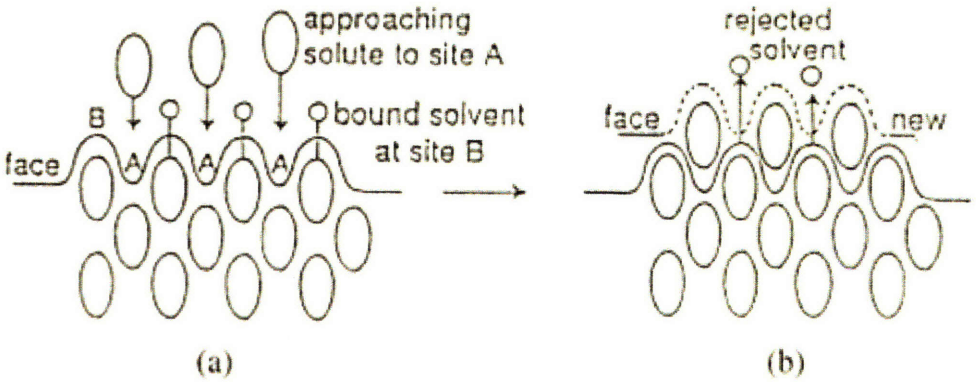


Figure 2-7: A schematic representation of *"relay type"* growth mechanism.

These models help in understanding the polymorph selection and morphology control of the final crystal. The Growth Synthon hypothesis helps in analyzing the polymorphic selection in some systems. The crystal growth models are also helpful

in explaining the inhibition of certain crystal forms even though they are the most stable under the given experimental conditions. Hence it is important to realize that polymorph selection in solvents can occur at both nucleation and growth stages. The next chapter introduces the solvent effects on glycine crystallization. This thesis is primarily concerned with using the above mentioned theories in understanding glycine polymorph selection in water-methanol solutions.

# Chapter 3

# Glycine Polymorphism

## 3.1 Glycine and its Polymorphs

The glycine model system is explored in this study to gain molecular level insights into the solvent effects on polymorphism. Glycine is not only chosen for its molecular simplicity and the abundance of experimental results in the literature but also due to its interesting polymorphic behavior in solutions. Three crystalline polymorphs were described for glycine: two monoclinic ($\alpha$, s.gr. P21/n, and $\beta$, s.gr. P21) and one trigonal ($\gamma$, s.gr. P31). The three polymorphs differ with respect to the connectivity between zwitterions ($NH_3{}^+$–$CH_2$–$COO^-$) [52].

The first attempts to study $\alpha$-glycine by means of X-ray diffraction were undertaken by Bernal [53] and by Hengstenberg and Lenel [54] independently. The explicit crystalline structure was refined by Albrecht and Corey [55], and a precise refinement of not only the heavier atoms but also locating of the hydrogen atoms for $\alpha$-modification was carried out by Marsh [56]. In the $\alpha$-polymorph the zwitterions are linked by hydrogen bonds in double anti-parallel layers, the interactions between these double layers being purely van der Waals as shown in Figure 3-1.

$\beta$-glycine had already been obtained and described by Fischer [57] at the beginning of the century, whereas X-ray examination was performed quite a long time later [58]. It was suspected that this fact was due to the general low stability of this phase and possibly due to irreversible transformation into $\alpha$ or $\gamma$-glycine forms. In the

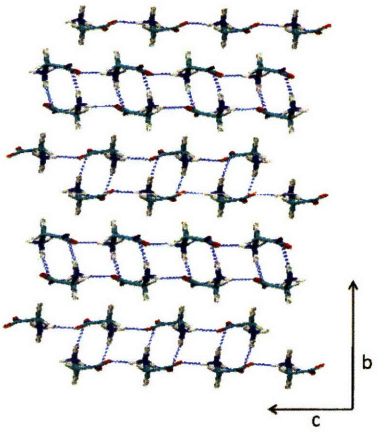


Figure 3-1: $\alpha$-glycine as viewed down the $a$-axis. Crystal consists of hydrogen bonded bilayers.

$\beta$-polymorph individual parallel polar layers are linked by hydrogen bonds in a three-dimensional network (Figure 3-2).

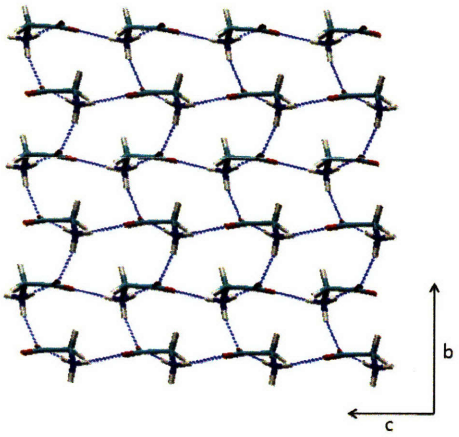


Figure 3-2: $\beta$-glycine crystal structure as viewed along the $a$-axis illustrating the three-dimensional hydrogen bond network.

The structure of $\gamma$-glycine was first revealed and resolved by X-ray diffraction by Iitaka [59–61]. Moreover, he analyzed not only the packing of the molecules in the crystal lattice, but also the role of the hydrogen bonds in the formation of the framework and the substructure of the hydrogen bonds. Investigations of $\gamma$-glycine at 298 and 83 K were carried out by means of neutron diffraction by Kvick [62] in order to determine electron density changes of the molecules with temperature. The

$\gamma$-polymorph consists of polar helices linked with each other in a three-dimensional polar network (Figure 3-3).

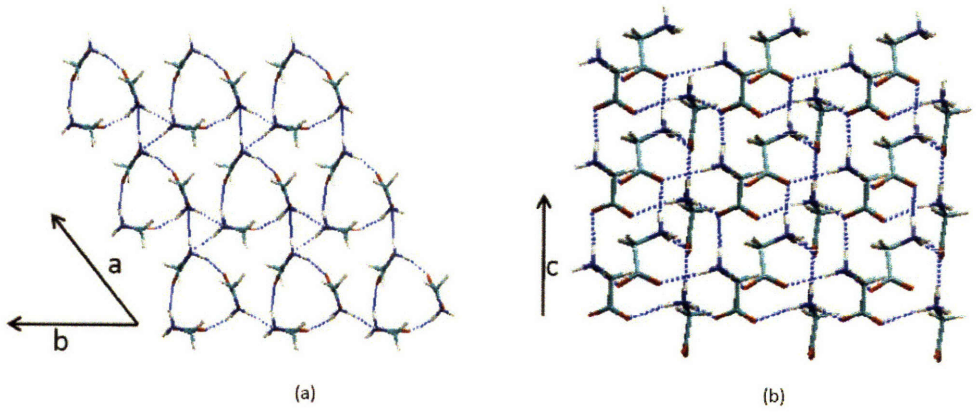


Figure 3-3: $\gamma$-glycine crystal structure.($a$) viewed down $c$-axis, ($b$) viewed parallel to $c$-axis. The crystal consists of polar helical hydrogen bond structure

The $\gamma$-polymorph is the most stable form at ambient conditions, although the $\alpha$-form crystallizes much more readily, and the $\alpha$-form (with rare exceptions) was not observed to transform into the $\gamma$-form at these conditions. With increasing temperature, the order of stability inverts, the $\alpha$-form becomes the most stable one above ~440 K, and a $\gamma \rightarrow \alpha$ polymorph transition is observed when the $\gamma$-form is heated. On subsequent cooling, the $\alpha$-form does not transform back to the $\gamma$-form, presumably due to kinetic reasons. The $\beta$-form is obviously metastable at all temperatures [53].

## 3.2 Solvent Effects on Glycine Polymorphism

Experimentally, the unusual feature of this system is that crystallization from aqueous solution at the natural isoelectric pH (5.97) always gives the $\alpha$ polymorph and it seems that under these conditions $\gamma$ never appears, despite its thermodynamic stability. It has been previously concluded that the nucleation and apparent 'stability' of the metastable $\alpha$ form at pHs close to the isoelectric point is a reflection of the presence of centrosymmetric dimer 'growth units' (see section 2.2.2) in solutions. On the basis

of solution [63], interfacial and solid-state chemistry [64] it was suggested that at and around the isoelectric point, glycine is dimerized in solution as centrosymmetric pairs of zwitterions. Myerson and Lo predicted that glycine exists mostly as dimers in supersaturated solutions by measuring the diffusion coefficient for supersaturated aqueous solutions of glycine [65]. Using small-angle X-ray scattering, Chattopadhyay et al. have directly studied the nucleation of the amino acid glycine from its aqueous supersaturated solution and indicated that glycine molecules exist as dimers in the supersaturated solution [33]. It is then apparent that nucleation from such solutions could lead directly and spontaneously to the metastable $\alpha$ structure [14]. This is further supported by the experiments involving S-control (supersaturation control) by Chew et al. where they have shown that $\alpha$-glycine grows about 500 times faster than $\gamma$-glycine in neutral aqueous solutions. This difference in growth rate corresponds to a difference in activation energy for growth of $\sim$15kJ $mol^{-1}$ calculated from the Arrhenius equation. This large difference in activation energy is attributed with the dissociation of Glycine dimers in solution prior to growth of $\gamma$-glycine, but their preservation in the $\alpha$-glycine crystal structure [66].

The next interesting issue is why $\gamma$-glycine forms at low pH aqueous solutions. In each of its polymorphic forms glycine molecules pack as zwitterions. As discussed above, the 'stability' of the metastable $\alpha$ form at pH close to the isoelectric point is a reflection of the presence of centrosymmetric dimer 'growth units' in solutions. The effect of moving the pH away from the isoelectric point is in reducing the proportion of the $\alpha$-form 'growth unit' (because singly charged glycine molecules will not form cyclic dimers). This would then increase the proportion of monomeric zwitterions available to form the polar chain structure of the $\gamma$-polymorph.

In the following thesis, precipitation of the least stable $\beta$-glycine from (50% v/v) methanol-aqueous solutions has been addressed from a molecular standpoint. The experimental results and underlying hypothesis (from literature) is discussed in the next section.

## 3.3 Glycine Polymorph Selections in Water–Methanol Solutions

As discussed previously, $\alpha$-glycine crystallizes primarily in aqueous solutions through hydrogen-bonded cyclic dimer growth units. The precipitation of $\gamma$-glycine at low or high pH aqueous solutions has been explained successfully by Davey et al. [67]. Another interesting case of polymorphic selection of glycine is the precipitation of $\beta$-glycine in alcohol-water solutions. The conundrum that the more thermodynamically stable $\alpha$- and $\gamma$-glycine polymorphs do not generally precipitate in aqueous solutions containing methanol or ethanol under the specified experimental conditions was addressed from the growth kinetics of the three polymorphs of glycine coupled with an analysis of the action of the solvent at the various crystal faces by Weissbuch et al. [4].

### 3.3.1 Precipitation of $\beta$-glycine

The first crystallization of $\beta$-glycine from water–alcohol solutions was reported by Fischer [57]. The crystal structure [58] is polar (space group P21) and comprises hydrogen-bonded layers, which are similar to those observed in the $\alpha$ form, but which are interlinked by NH$\cdots$O and CH$\cdots$O interactions through a twofold screw-symmetry axis perpendicular to the layer plane (Figure 3-2). The addition of alcohol reduces the solubility of glycine from 25.0 g/100 mL water (25 °C) to 2.65 g/100 mL solvent in 50.1%(v/v) ethanol-water mixtures. It was hypothesized that this reduced solubility would result in an increased concentration of solvated glycine monomers relative to that of hydrogen-bonded cyclic dimers. Such behavior is apparently consistent with the preferred precipitation of $\beta$-glycine from alcohol–water solutions because the crystal structure consists of hydrogen-bonded monomer units, as opposed to $\alpha$-glycine which comprises cyclic hydrogen-bonded pairs.

Long needles of $\beta$-glycine were grown in water–ethanol mixtures containing 50, 26.1, and 10% (v/v) ethanol and also from 1:1 water–methanol mixtures containing

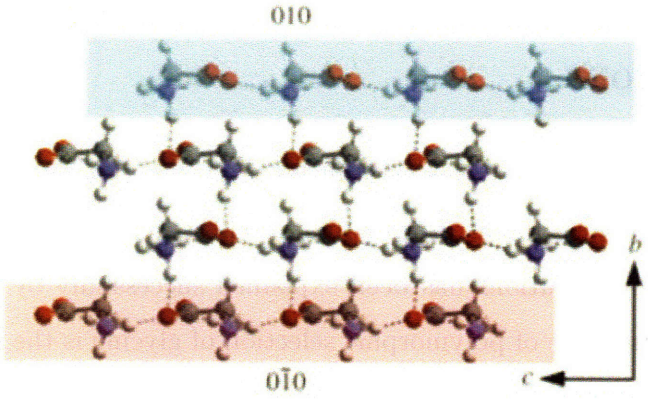


Figure 3-4: Packing arrangement of $\beta$-glycine. The (010) "azure" and (0$\bar{1}$0) "pink" surfaces, are exposed at the interface.[4]

4.0, 19.0, 35.9, and 5.0 g glycine/100 mL solvent, respectively. Growth kinetic measurements of single $\beta$-glycine crystals in 1:1 water-ethanol solutions at 25 °C reveal a fast growth at one pole of the needle and a very slow growth at the opposite end. The absolute polarity [68] of $\beta$-glycine was determined by employing "tailor-made" additives[5], in this case racemic tryptophane (Trp). It was concluded that $\beta$-glycine grows faster at the side with exposed C—H bonds (colored azure) than at the opposite side with exposed N—H bonds (colored pink; Figure 3-4). Previous studies have shown that the relative rates of growth at the opposite ends of polar crystals in polar solvents can be correlated directly with the relative rates by which solvent molecules are stripped from the opposite ends [49, 69–71]. The faster growth rate at the $\beta$-glycine pole with exposed C—H bonds is in agreement with this model; the water or alcohol solvent molecules can be attached more effectively to the slow growing glycine surface with exposed N—H bonds through strong $OH_{sol} \cdots O_{gly}{}^{-}$ and $NH_{gly}{}^{+} \cdots O_{sol}$ interactions than to the fast growing $\beta$-glycine pole with exposed C—H bonds with strong $OH_{sol} \cdots O_{gly}{}^{-}$ interactions but only weak $CH_{gly} \cdots O_{sol}$ interactions.

### 3.3.2 Inhibition of $\gamma$-glycine

The absence of the stable $\gamma$-glycine form in crystals formed in alcohol–water solutions is explained by examination of its growth properties (see section 2.3.2). The polar

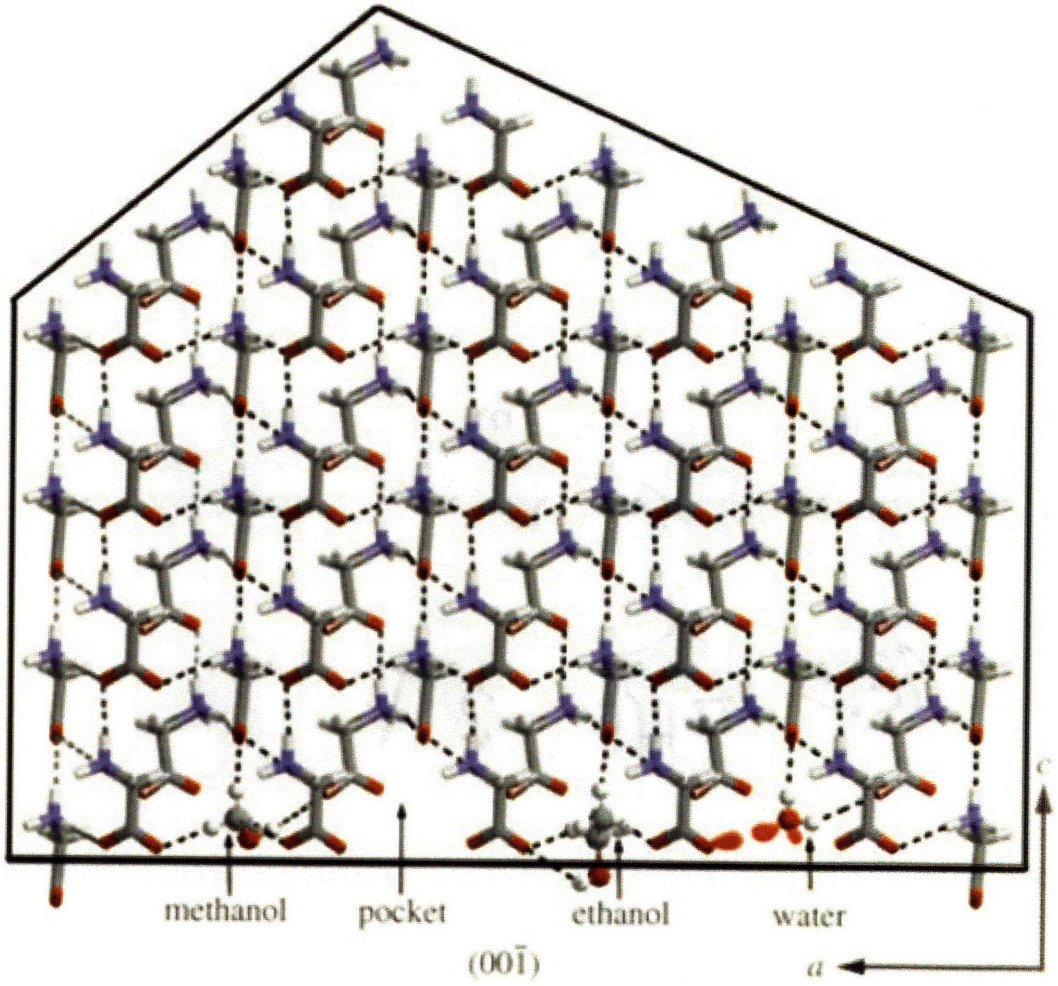


Figure 3-5: Packing arrangement of $\gamma$-glycine showing the pockets of fast growing (00$\bar{1}$) face that are poisoned by the adsorption of ethanol and methanol molecules (shown as "balls and sticks").[4]

crystal structure of $\gamma$-glycine (space group P31; Figure 3-3), which is not composed of cyclic glycine pairs, is delineated by a (00$\bar{1}$) face at which $CO_2^-$ groups emerge and capped crystal faces at the opposite end that expose $NH_3^+$ groups. Previous studies [72] have shown that $\gamma$-glycine, grown in aqueous solutions and in the presence of auxiliaries that inhibit the crystallization of $\alpha$-glycine, appear as [001] needles that grow along the polar $c$ axis much faster at the end of the crystal with the $CO_2^-$

groups than at the opposite capped end. This unidirectional growth was interpreted in terms of a "relay" mechanism as described in section 2.3.2. However, ethanol and methanol solvent molecules can reside within the pockets through $OH_{sol} \cdots O_{gly}{}^{-}$ and $CH_{alcohol} \cdots O_{gly}{}^{-}$ hydrogen-bonding interactions, thus inhibiting growth at the $CO_2{}^{-}$ end of the crystal (Figure 3-5). In several of the crystallization experiments carried out in water-ethanol mixtures, the few $\gamma$-glycine crystals that were observed exhibited morphology in keeping with the proposed inhibition by ethanol or methanol of growth along the otherwise fast growing $CO_2{}^{-}$ end of the crystal (Figure 3-6).

Figure 3-6: $\gamma$-glycine crystals observed in several crystallizations from a 1:1 water–ethanol solution.[4]

### 3.3.3 Inhibition of $\alpha$-glycine

The surface of the fast and slow growing ends of $\alpha$-glycine are very similar in structure to the {010} surfaces of $\beta$-glycine with either exposed C—H or N—H bonds, as shown in (Figure 3-7) respectively. On the basis of the realistic assumption, which is supported by experimental evidence [64, 73], that glycine molecules in aqueous solution dock onto the crystal surface primarily as hydrogen-bonded cyclic glycine pairs, it is thought that a {010} face will expose the faster growing surface with exposed C—H bonds to a much larger extent than the slower growing surface with exposed N—H bonds.

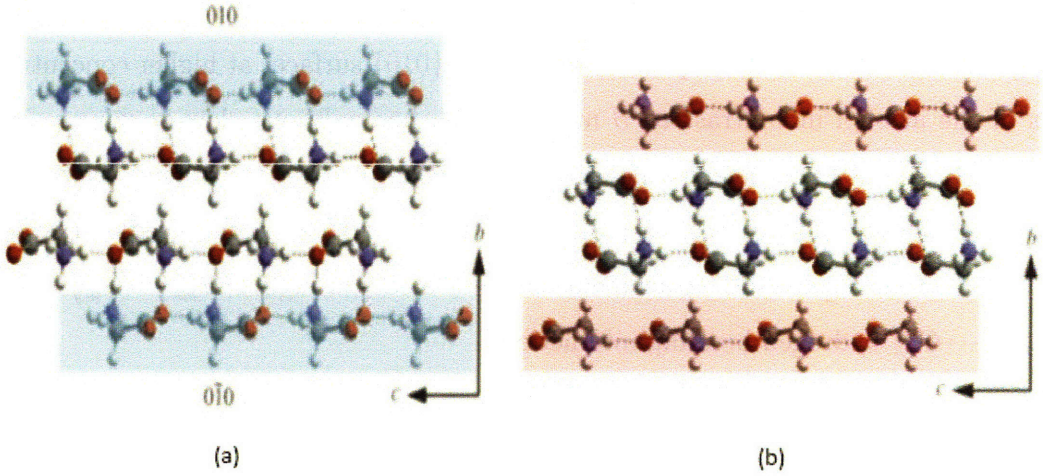


Figure 3-7: Packing arrangements of $\alpha$-glycine ($a$) exposing weak solvent binding C—H bonds to the solution at (010) surface (azure) or ($b$) exposing strong solvent-binding N—H bonds to the solution at the (010) surface (pink).[4]

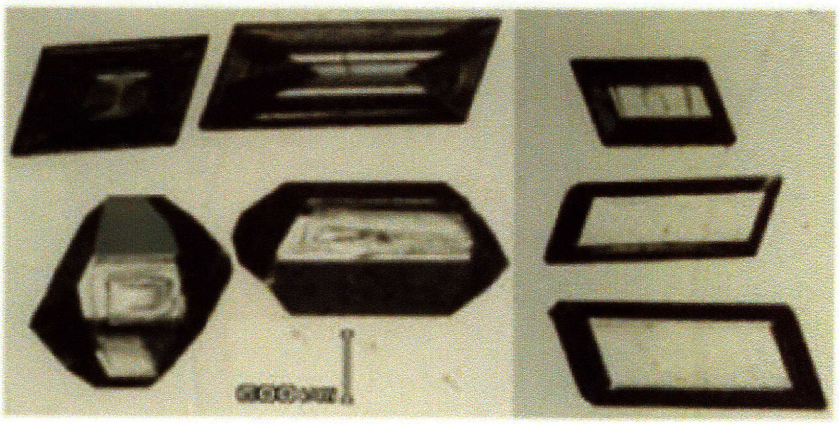

Figure 3-8: $\alpha$-glycine crystals grown from 9:1 water-ethanol.[4]

It was anticipated that reduced solubility of glycine in solution caused by the presence of alcohol would lead to a higher proportion of solvated glycine monomer units docking onto the $\alpha$-glycine {010} surface sites with exposed N—H bonds. Thus, the time required to strip the overlying solvent molecules, prior to formation of the glycine cyclic dimer growth units and propagation of the glycine bilayer with exposed C—H bonds on its {010} surface, would lead to an overall reduction in growth rate along the $\pm$b directions of the $\alpha$-glycine crystal. Indeed, the $\alpha$-glycine crystals obtained from a 9:1 water-ethanol solution tended to display more well developed {010}

faces (Figure 3-8) than crystals obtained from purely aqueous solutions. Therefore, embryonic crystallites would expose slow-growing {010} surfaces at higher concentrations of the alcohol in contrast to $\beta$ nuclei, which has only one slow-growing polar end and so results in a preferred kinetic precipitation of the latter. Thus, water or alcohol as solvent impedes growth normal on the {h0l} faces of the needle crystals as a result of strong solvent attachment to these faces through $OH_{sol} \cdots O_{gly}{}^{-}$ and $NH_{gly}{}^{+} \cdots O_{sol}$ hydrogen bonding interactions.

# Chapter 4

# Validation of Force Field Parameters

It is necessary to have the right force field and parameters for performing molecular dynamic simulations of glycine solutions and interfaces. The force field consists of intramolecular parameters (defining the bonds, angles, dihedrals and impropers), Lennard-Jones terms for the dispersion energy between atoms and the partial charges for electrostatic interactions. The validity of a particular force field and the parameters has to be tested both for solid state and solution behaviour. For solid state, the lattice parameters of the three glycine polymorphs and the enthalpy of sublimation are compared with their corresponding experimental values. For solution behavior, water coordination numbers and distances are calculated and compared with experimental values obtained from neutron diffraction measurements.

The experimental crystal structures and lattice parameters of the three glycine polymorphs are obtained from the Cambridge Structural Database (CSD) [74]. The experimental lattice parameters of glycine polymorphs are tabulated in Table 4.2. Using the coordinates obtained from the CSD, minimization and dynamics of the polymorphs were performed in NAMD [75] with periodic boundary conditions using CHARMM [76], OPLS [77], and AMBER [78] force fields. Ewald summation [79] is employed for the electrostatics. The number of unit cells and atoms that comprise the supercell used in periodic boundary conditions is shown in Table 4.3. Only OPLS was successful in maintaining a stable crystal structure of all the three polymorphs. AMBER and CHARMM failed to maintain the stability of $\alpha$ and $\gamma$ glycine polymorphs.

The OPLS force field was further tested for its ability to reproduce experimental lattice parameters at room temperature using molecular dynamics simulations. Constant Pressure Molecular dynamics simulations of all the three polymorphs were carried out for 1ns at 300K and at 1 atmosphere pressure without applying any constraints on the supercell. Even though OPLS force field was successful in reproducing stable hydrogen bond networks in glycine polymorphs, the lattice parameters of $\alpha$-glycine showed large deviation ($\sim$ 8%) from experimenatally observed parameters. This is resolved by modifying the lennard jones parameters of the $\alpha$-hydrogen (H4 and H5) attached to $\alpha$ carbon (C1) in glycine zwitterion (Figure 4-1). The lennard-jones parameters for $\alpha$-hydrogen developed by Veenstra et. al. [80] and implemented in AMBER forcefield for glycine zwitterion were used in this study. The OPLS LJ parameters and the parameters used in this study are tabulated in Table 4.1. Shown in Table 4.4 are the root mean square deviations (RMSD) of the minimized crystal structures using the modified OPLS parameters. Table 4.5 shows the percentage deviation in lattice parameters of the three polymorphs during the 1 nanosecond simulation. The crystal structures and the hydrogen bond networks in the polymorphs were successfully maintained during the dynamics.

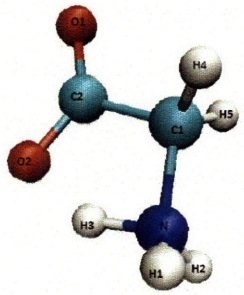


Figure 4-1: Glycine zwitterion with all the atoms labeled. The lennard-jones parameters of H4 & H5 were modified to obtain a better agreement with experimental observations.

Table 4.1: Lennard Jones parameters for $\alpha$-hydrogen.

| Parameters | $\epsilon_{min}$ (kcal/mol) | $R_{min}$ Å |
|---|---|---|
| OPLS | -0.0300 | 1.4031 |
| Modified [80] | -0.0157 | 1.1000 |

Table 4.2: Polymorph Details for Glycine

| Polymorph | Lattice Type | Lattice Parameters |
|---|---|---|
| $\gamma$-glycine | Trigonal $P31$ | $a = 7.046$, $b = 7.046$, $c = 5.491$<br>$\alpha = 90$, $\beta = 90$, $\gamma = 120$. |
| $\alpha$-glycine | Monoclinic $P21/n$ | $a = 5.1054$, $b = 11.9688$, $c = 5.4645$<br>$\alpha = 90$, $\beta = 111.70$, $\gamma = 90$. |
| $\beta$-glycine | Trigonal $P21$ | $a = 5.0932$, $b = 6.270$, $c = 5.3852$<br>$\alpha = 90$, $\beta = 113.19$, $\gamma = 90$. |

Table 4.3: Number of Unit Cells and molecules per super cell during minimization runs.

| Polymorph | Supercell Size | Number of Molecules in the supercell |
|---|---|---|
| $\gamma$-glycine | $5X5X6$ unit cells<br>$(35.23X35.23X32.95)$ Å$^3$ | 450 molecules |
| $\alpha$-glycine | $6X3X6$ unit cells<br>$(30.63X35.91X32.79)$ Å$^3$ | 432 molecules |
| $\beta$-glycine | $7X5X7$ unit cells<br>$(35.65X31.36X37.70)$ Å$^3$ | 490 molecules |

Table 4.4: Root Mean Square Deviation (RMSD) of glycine polymorphs during minimization using OPLS force field.

| Polymorph | RMSD |
|---|---|
| $\alpha$-glycine | 0.393 |
| $\beta$-glycine | 0.285 |
| $\gamma$-glycine | 0.236 |

Table 4.5: Percentage Deviation of lattice parameters of the three polymorphs of glycine during a 1nanosecond molecular dynamics simulation at 300 K with OPLS force field

| Polymorph | % Deviation of Lengths | % Deviation of Angles |
|---|---|---|
| $\alpha$-glycine | $a$ = -2.09%,<br>$b$ = 2.803%, $c$ = -3.74%. | $\alpha = 0\%$,<br>$\beta$ = +0.35%, $\gamma = 0\%$. |
| $\beta$-glycine | $a$ = -2.9%,<br>$b$ = 4.42%, $c$ = -4.14%. | $\alpha = 0\%$,<br>$\beta$ = +0.5%, $\gamma = 0\%$. |
| $\gamma$-glycine | $a$ = -0.63%,<br>$b$ = -0.66%, $c$ = 2.64%. | $\alpha = 0\%$,<br>$\beta = 0\%$, $\gamma = 0\%$. |

The lattice energies of the glycine polymorphs at Zero Kelvin are tabulated (Table 4.6). The difference in potential energies obtained are qualitatively in good agreement with those calculated using DFT [81]. The calculated enthalpy of sublimation

Table 4.6: Relative lattice energies of glycine polymorphs obtained by annealing the crystals to Zero Kelvin.

| Polymorph | Lattice Energy(kcal/mol) | Relative Energy (kcal/mol) |
|---|---|---|
| $\alpha$-glycine | -176.32 | 0.0 |
| $\beta$-glycine | -175.24 | +1.08 |
| $\gamma$-glycine | -175.14 | +1.18 |

for glycine using the method illustrated by Bisker-Leib and Doherty [82] is $\sim$ 34.3 kcal/mol. This is in close agreement with the experimental enthalpy of sublimation which is 32.6 $\pm$ 0.5 kcal/mol. The OPLS parameters with modified hydrogen lennard-jones parameters were further tested for their ability to model glycine-water interactions. The radial distribution functions are calculated for selected atoms in glycine with the oxygen atoms ($O_w$) of water molecules. Kameda et al. [83] performed neutron diffraction measurements and showed that the ammonium group of glycine in 5.0 M aqueous solution is coordinated to 3.0 $\pm$ 0.6 water molecules and the distance between nitrogen atom in glycine and oxygen atom in water is 2.85 $\pm$ 0.5 Å. $g(r)$ between nitrogen and oxygen atom in water is shown in Figure 4-2. The OPLS parameters with modified $\alpha$-hydrogen parameters give a coordination number of $\sim$ 3.0 and a $N_{gly}$—$O_w$ distance of $\sim$ 2.89 Å. Also shown is the $g(r)$ (Figure 4-3) between the ammonium hydrogen of glycine and the oxygen atom of water.

Similar calculations were performed for the carboxylate group of glycine. A coordination number of $\sim$ 4.9 and a $O_{gly}$—$O_w$ distance of $\sim$ 2.67 Å is obtained (Figure 4-4). A previous ab initio study [84] found that the number of water molecules in the first hydration shell is $\sim$ 4.7. A good agreement between the computational and experimental results bolsters our confidence in the interatomic force fields used. These parameters are a good fit to model the solid state, interfacial and solution behavior of glycine. Tabulated (Tables 4.7 and 4.8) below is a comparison between coordination numbers and distances calculated with the available experimental and ab initio results.

Table 4.7: Average Coordination numbers with oxygen atoms in water.

| Atoms | Calculated | Experimental | Ab Initio |
|---|---|---|---|
| $N_{gly}$— $O_w$ | 3.0 | 3.00 ± 0.6 [83] | 3.0 [84] |
| $O_{gly}$— $O_w$ | 4.9 | – | 4.7 [84] |

Table 4.8: Average Atom - Atom Distance

| Atoms | Calculated | Experimental | Ab Initio |
|---|---|---|---|
| $N_{gly}$— $O_w$ | 2.89 | 2.85 ± 0.05 [83] | 2.75 [84] |
| $O_{gly}$— $O_w$ | 2.67 | – | – |

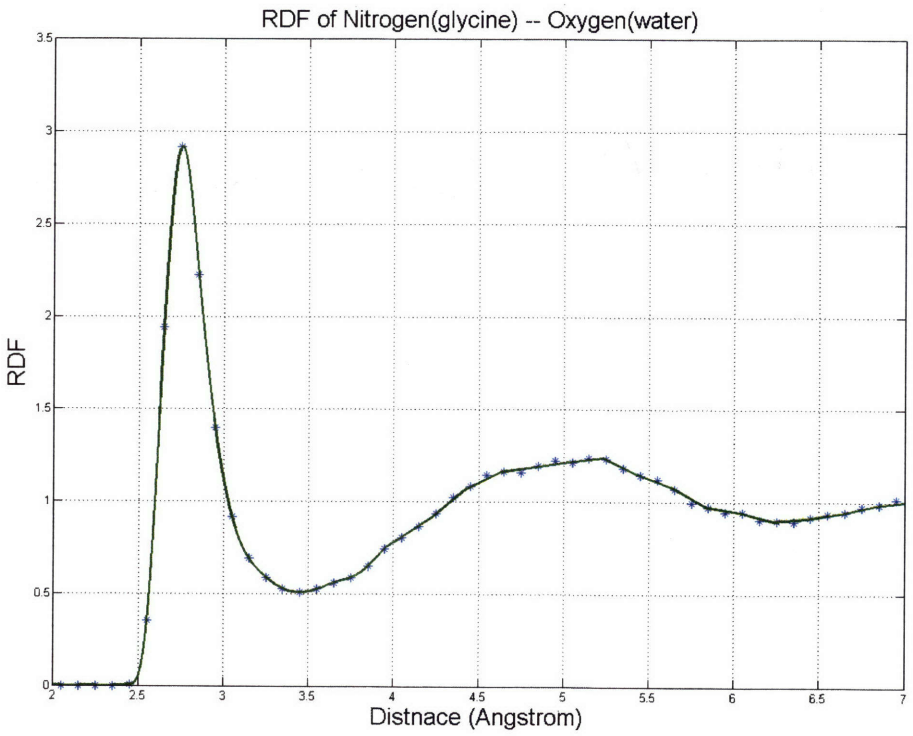


Figure 4-2: Radial distribution function calculated for the nitrogen atom in glycine and oxygen atom in water.

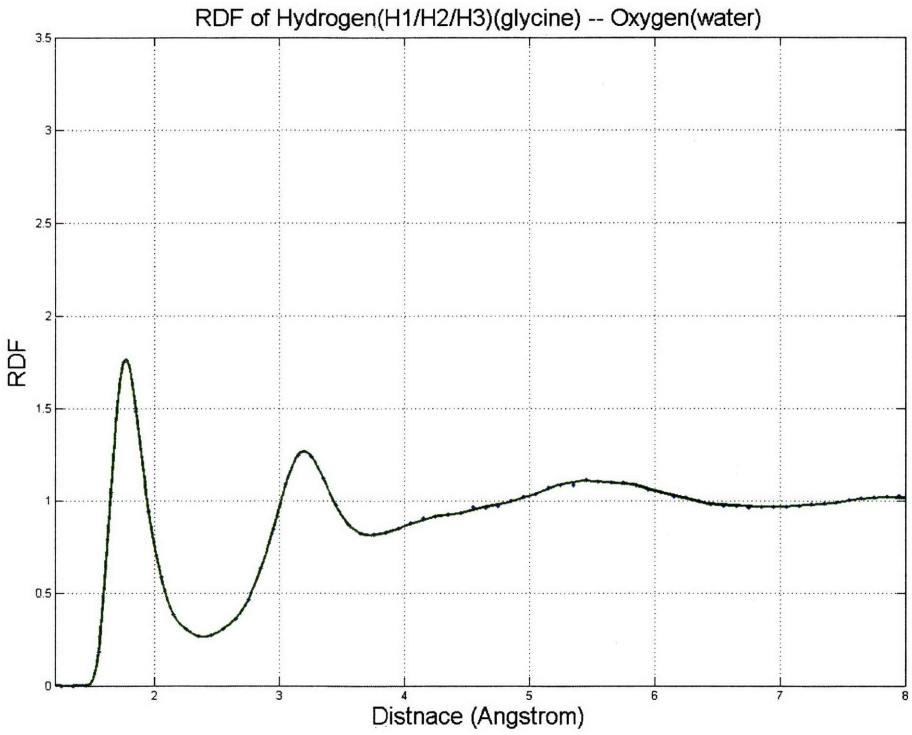


Figure 4-3: Radial distribution function calculated for the hydrogen atom attached to nitrogen in glycine and oxygen atom in water.

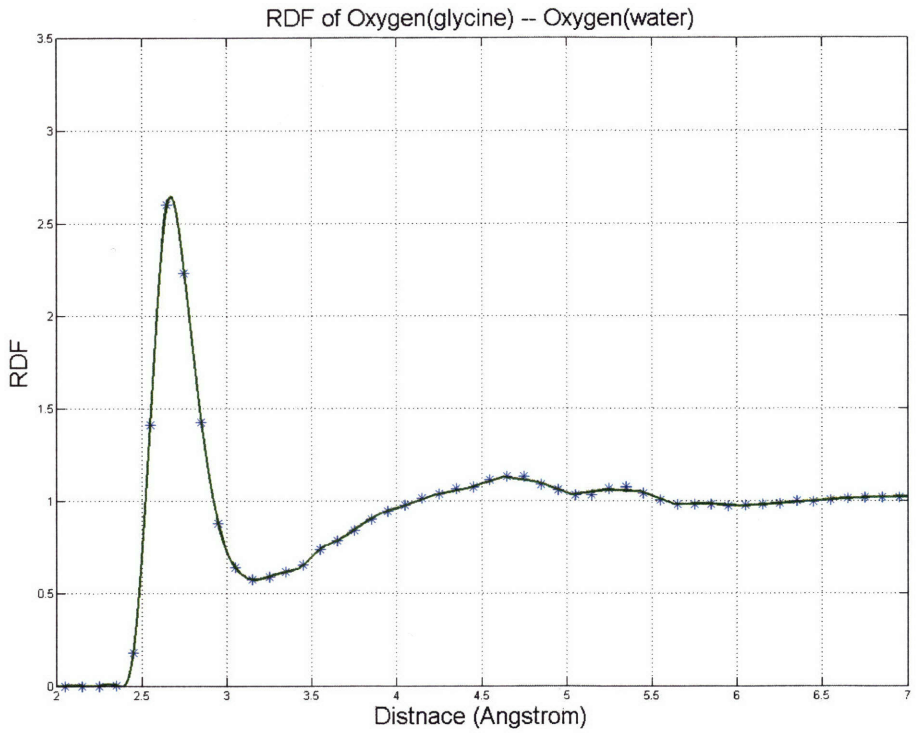


Figure 4-4: Radial distribution function calculated for the oxygen atom in glycine and oxygen atom in water.

# Chapter 5

# Simulation Methods & Results

## 5.1 Solution Behavior of Glycine

The hypothesis suggested for $\beta$-glycine crystallization from water-methanol solutions by Weissbuch et al. revolves around the assumption that non-dimer like units dock onto the (010) interface of $\alpha$-glycine during its growth. This exposes the N—H groups at the interface which further inhibit crystal growth of $\alpha$-glycine. Simulations of solution behavior of glycine in water and water-methanol solutions have been carried out to explore the possibility of decrease in dimer like structures ('growth units' for $\alpha$-glycine). Initially, the stability of a dimer structure is tested by calculating the lifetimes of a glycine dimer unit in water and water-methanol solutions. Free energy of the dimerization reaction was then computed by the Umbrella Sampling method. Further simulations were carried out to compute the fraction of glycine molecules that exists as monomers and dimers in water and 50% v/v water-methanol solutions with varying supersaturations.

### 5.1.1 Dimer Lifetime

Simulations with glycine dimer structure (shown in Figure 5-1) as the starting configuration were carried out in water and water-methanol solutions. The concentration of methanol in the solution is 0.3088 mole fraction (which corresponds to 50% v/v water-

methanol mixture). Constant Volume and Temperature (NVT) Molecular Dynamics simulations in a 28 Å box were carried out for 0.5 nanosecond. Four simulations each in water and water-methanol solvents with different initial velocities were carried out to explore the stability of the dimer structure. The average of distances $d1$ and $d2$ (Figure 5-1) is plotted with time. The plots suggest higher lifetime of the centrosymmetric dimer structure in water-methanol solutions. But to be able to make any accurate conclusions about the relative stability of the dimer structure in water-methanol mixtures it is necessary to calculate the relative free energies.

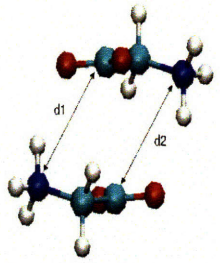


Figure 5-1: Dimer Structure of Glycine.

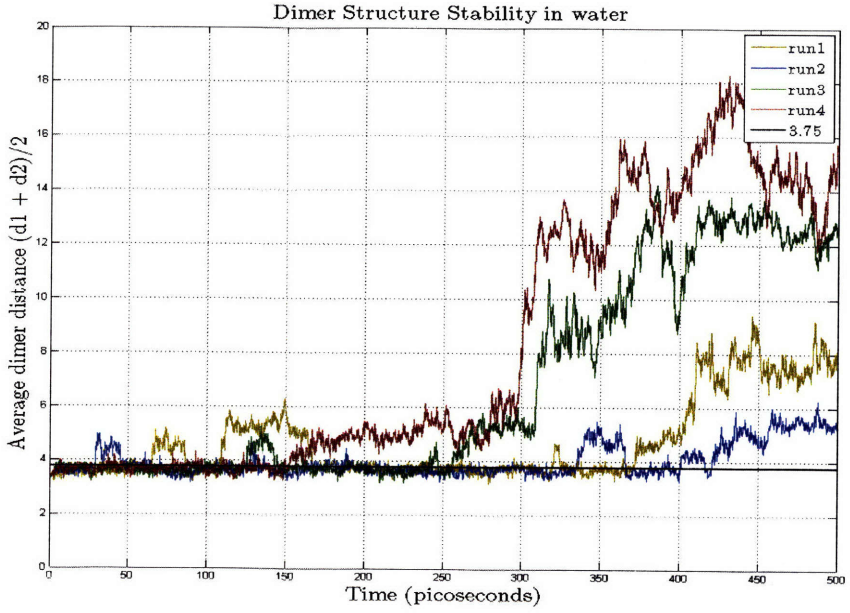


Figure 5-2: Illustration of lifetimes of Dimer Structure in Water. The dark line at 3.75 Å represents the average $(d1 + d2)/2$ for the dimer structure.

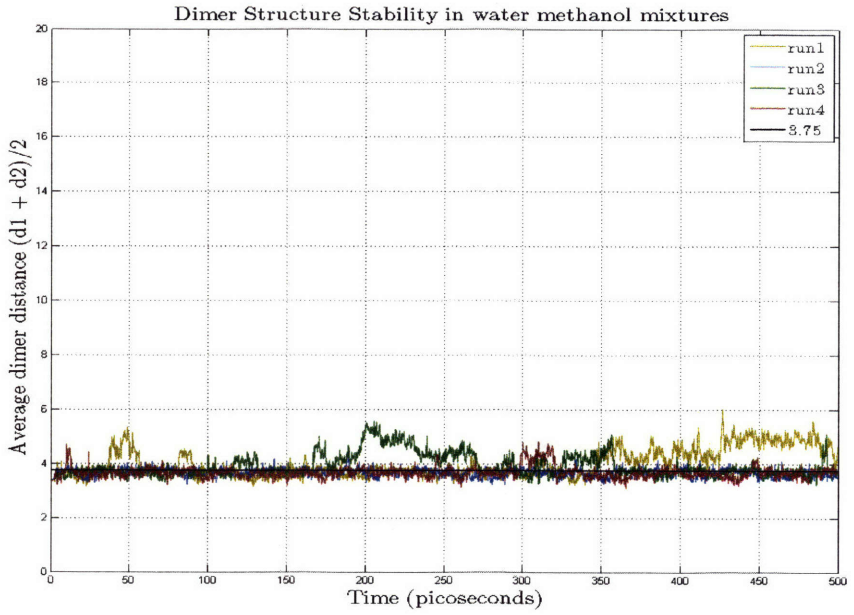


Figure 5-3: Illustration of lifetimes of Dimer Structure in Water-Methanol mixtures. The dark line at 3.75 Å represents the average $(d1 + d2)/2$ for the dimer structure.

### 5.1.2 Free Energy Calculations

Potential Mean Force (PMF) calculations were performed to compare the relative stability of a dimer in water and water-methanol mixtures. MD Umbrella Sampling [6] was used to obtain a free energy profile for the dimerization reaction. Shown below in Figure 5-4 is the free energy diagram for the formation of a dimer structure with two hydrogen bonds from glycine monomers. The reaction coordinate was assumed to be the average of the distances $d1$ and $d2$ shown Figure 5-1. A harmonic umbrella potential ($k = (k_o/2)(\delta - \delta_o)^2$) is applied along the reaction coordinate at an interval of 0.25 Å. The system consisted of two glycine molecules in a 28 Å cubic box. Constant Volume and Temperature Molecular Dynamics were performed at 300 Kelvin.

As can be observed from the free energy plots the centrosymmetric dimer structure is more stable ($\sim$ 1 kcal/mol) in water-methanol solutions. Even the activation energy for dissociation of the dimer structure is higher ($\sim$0.2 kcal/mol) in 50% v/v solution of water-methanol than in pure water. Even though the magnitude of the differences in free energies is relatively insignificant compared to the thermal fluctuation

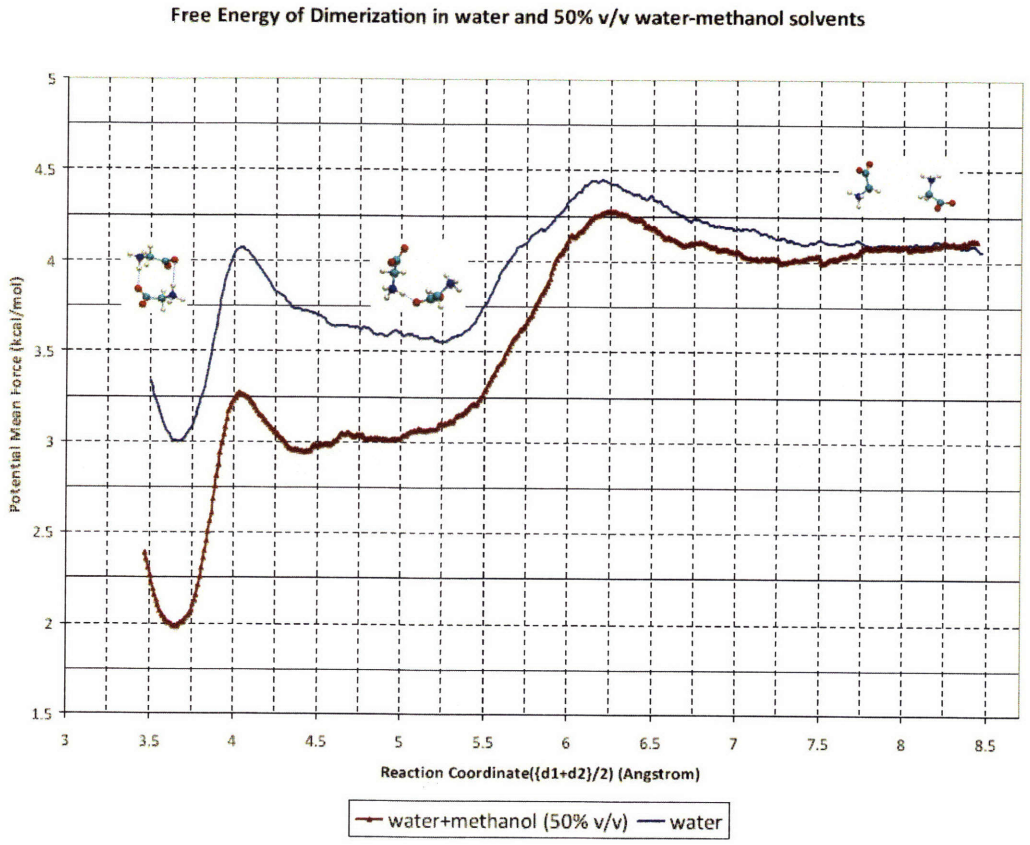


Figure 5-4: Free Energy diagram of dimerization in water and 50% v/v water-methanol solvents.

energies, it is concluded that the dimer structure is more stable in 50% v/v water-methanol mixtures than in pure water solutions. The fact that the solubility of glycine is much lower in water-methanol solvents than in water provides further evidence for the higher stability of dimer structure in water-methanol solutions. This result seemingly condradicts the hypothesis of existence of more monomer-like structures in water-methanol solutions. The solution behavior is further explored by analyzing the fraction of glycine molecules that exist as monomers and dimers in solutions of glycine in water and 50% v/v water-methanol solutions at various supersaturations.

## 5.2 Solution Simulations of Glycine

Solutions of Glycine in water and 50% v/v water-methanol mixtures at various supersaturation ratios were simulated in NAMD. Supersaturatio ratio is defined as $(C - C_s)/C_s$, where $C$ is the concentration of glycine in the solution and $C_s$ is the solubility limit in the solution. Concentrations are expressed as mole ratios, i.e. number of moles of solute devided by the number of moles of solvent. Solubility of Glycine in water is 0.059 mole ratio (0.059 moles of glycine in one mole of water) and in 50% v/v water-methanol mixture is 0.0088 mole ratio (0.0088 moles of glycine in 0.6912 moles of water and 0.3088 moles of methanol). Show below in Tables 5.1 and 5.2 are the various supersaturations and number of molecules of each component in the solutions used in the simulations.

Table 5.1: System Details for glycine-water solutions.

| Concentration | $(C - C_s)/C_s$ | Number of Glycine | Number of Water |
|---|---|---|---|
| 0.0297 | -0.5 | 100 | 3367 |
| 0.0445 | -0.25 | 200 | 4489 |
| 0.0535 | -0.1 | 200 | 3741 |
| 0.0653 | +0.1 | 200 | 3061 |
| 0.0891 | +0.5 | 300 | 3367 |
| 0.1188 | +1 | 400 | 3367 |

These systems were simulated for four nanoseconds and the trajectories of the last nanosecond were analyzed to find the extent of aggregation and the fraction of molecules that exists as monomers and dimers in the solution. Geometric criterion for defining a hydrogen bond is thoroughly tested for the solutions simulated. The crystal structure of $\alpha$-glycine consists of a centrosymmetric dimer unit (Figure 5-1) with a $H_{gly} \cdots O_{gly}$ distance of 2.1 Åand an $N_{gly}$—$H_{gly} \cdots O_{gly}$ angle of 154°. A cut-off of 2.2 Å and 140° was found to be an optimal definition for hydrogen bond between glycine. This same definition was used in a previous study by Hughes et al. [85] for hydrogen bonding between glycine zwitterions in water. Figures 5-5 and 5-6 show the variation of the fraction of glycine monomers with time in water and water-methanol mixtures respectively.

Table 5.2: System Details for glycine-water-methanol solutions.

| Concentration | $(C - C_s)/C_s$ | Number of Glycine | Number of Water | Number of Methanol |
|---|---|---|---|---|
| 0.0044 | -0.5 | 50 | 7855 | 3509 |
| 0.0066 | -0.25 | 75 | 7855 | 3509 |
| 0.0079 | -0.1 | 75 | 6545 | 2924 |
| 0.0097 | +0.1 | 75 | 5355 | 2393 |
| 0.0132 | +0.5 | 100 | 5236 | 2339 |
| 0.0176 | +1 | 150 | 5891 | 2623 |

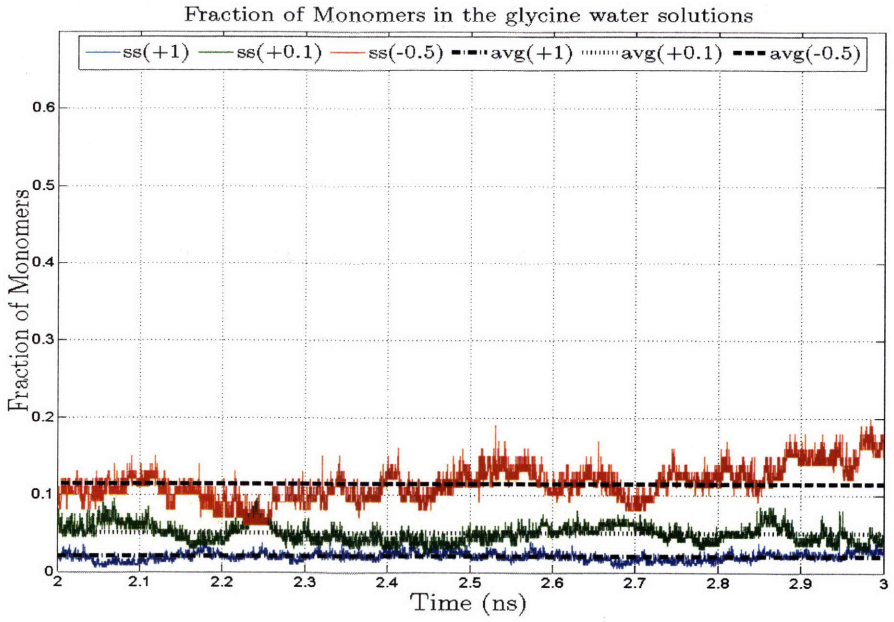


Figure 5-5: Fraction of glycine molecules that exist as monomers in glycine water solutions at three different concentrations is shown. The thick lines correspond to the average fraction of monomers.

Figure 5-7 shows the fraction of glycine molecules that exist as monomers in water and water-methanol mixtures at various supersaturations studied. Clearly as the supersaturation is increased the number of monomers decreases in the both solvents. Interestingly, we observed a higher fraction of monomers in 50% v/v water-methanol mixture than in water. This result supports the hypothesis of the presence of higher percentage of monomers in water-methanol mixtures and might seem inconsistent with the free energy calculations which predict a higher stability of dimers in the

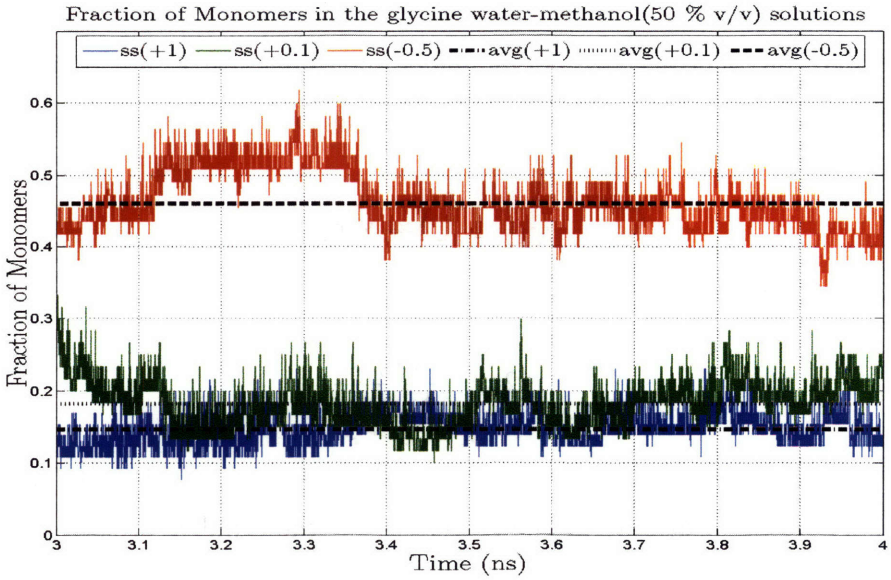


Figure 5-6: Fraction of glycine molecules that exist as monomers in glycine water-methanol solutions at three different concentrations is shown. The thick lines correspond to the average fraction of monomers.

presence of methanol additive. A simple equilibrium model is used with reasonable assumptions to show qualitatively why higher monomer concentration can be expected in water-methanol mixtures.

The dimerization reaction that occurs in the solution can be written as:

$2GLY_{monomer} \Longleftrightarrow Gly_{catamer} \Longleftrightarrow Gly_{dimer}$

The free energy diagram (Figure 5-4) is used to estimate the equilibrium constants for the reactions involved. The mass action law is used to caculate the approximate monomer fraction in the solutions.

$K1_{eq} = exp(\frac{-\Delta G1_{eq}}{kT}) = \frac{a_{catamers}}{a_{monomers}{}^2}$

$K2_{eq} = exp(\frac{-\Delta G2_{eq}}{kT}) = \frac{a_{dimers}}{a_{catamers}}$

Total number of glycine molecules can be expressed as,

$$N_{gly} = N_{gly,monomer} + 2N_{gly,catamer} + 2N_{gly,dimer} + \sum i(N_{gly,i^{th}aggregate})$$

$$\approx N_{gly,monomer} + 2N_{gly,catamer} + 2N_{gly,dimer} \quad (5.1)$$

For simplicity, we assume the number of glycine molecules present in higher ag-

gregates to be negligible. This assumption obviously breaks down at higher concentrations of glycine. The activities of monomer and dimer species are approximated to mole fractions which is a reasonable assumption at lower concentrations of glycine.

$$K1_{eq} = \frac{X_{catamer}}{X_{monomer}{}^2} \tag{5.2}$$

$$K2_{eq} = \frac{X_{dimers}}{X_{catamer}} \tag{5.3}$$

The mole fractions can be expressed as a function of supersaturation ratio 'S'. If the solubility limit of glycine in the solvent is $c_s$, the number of solvent molecules required to obtain a supersaturation ratio of $S$ is

$$N_{solvent} = \frac{N_{gly}}{c_s(1+S)} \tag{5.4}$$

$$X_{dimer} \approx \frac{(N_{gly,dimer})}{(N_{solvent})} \tag{5.5}$$

$$X_{catamer} \approx \frac{(N_{gly,catamer})}{(N_{solvent})} \tag{5.6}$$

$$X_{monomer} \approx \frac{(N_{gly,monomer})}{(N_{solvent})} \tag{5.7}$$

In Equations 5.5, 5.6 and 5.7 the number of glycine are assumed to much smaller than the number of solvent molecules. Solving equations 5.1 to 5.7, we obtain

$$K1_{eq}(1+K2_{eq}) = \frac{(1-f_{gly,monomer}))}{2(c_s(1+S))((f_{gly,monomer})^2)} \tag{5.8}$$

The above equation is solved for $f_{gly,monomer}$ in both water and water-methanol mixtures and is plotted against the supersaturation ratio (Figure 5-8). $\Delta G1_{eq}$ and $\Delta G2_{eq}$ are estimated using the dimerization free energy plots. As can be observed, the fraction of monomers is higher in the solvent with lower solubility and higher dimer stability. If the solubility is decreased and $\Delta$G for dimerization reaction is kept constant, the monomer fraction at the same supersaturation increases. Similarly if

the $\Delta G$ for dimerization reaction is slightly increased (made more negative) without changing the rest of the variables, the monomer fraction decreases. Therefore, at similar supersaturation levels both the solubility limit and free energy of dimerization play very important and opposing roles in governing monomer fraction of glycine in solutions. We speculate that the increase in monomer fraction in water-methanol mixtures stems from the fact that decrease in solubility is much larger than the corresponding increase in dimer stability.

Regarding the applicability of the equilibrium thermodynamics in this scenario, the actiavtion barrier for dimerization reaction is very low compared to thermal fluctuations and the diffusion of glycine in the solutions is reasonably high to reach quasi-equilibrium with respect to the dimerization reaction even though the solutions are supersaturated. But it is very important to note that the above equilibrium model gives only a qualitative picture beacuse of the various assumptions used which are valid only at very low concentrations of glycine. The large difference in calculated and predicted monomer fractions from the model should also be attributed to the presence of a major fraction of glycine molecules in higher order aggregates.

Shown in Figure 5-9 is the fraction of glycine molecules that exist as dimers (catamers & centrosymmetric dimers) in the solution. The plots show a relatively small number of glycine dimers in the solutions. The water-methanol solvents have a higher fraction of dimers at very low supersaturations but at higher supersaturation ratios the difference in dimer fractions is very small. The fraction of dimers in the solution does not increase with concentration of glycine. This unexpected behavior could be attributed to the presence of higher order aggregates where the interactions between the monomers, dimers and the aggregates also has to be considered. Future studies will focus on such interactions.

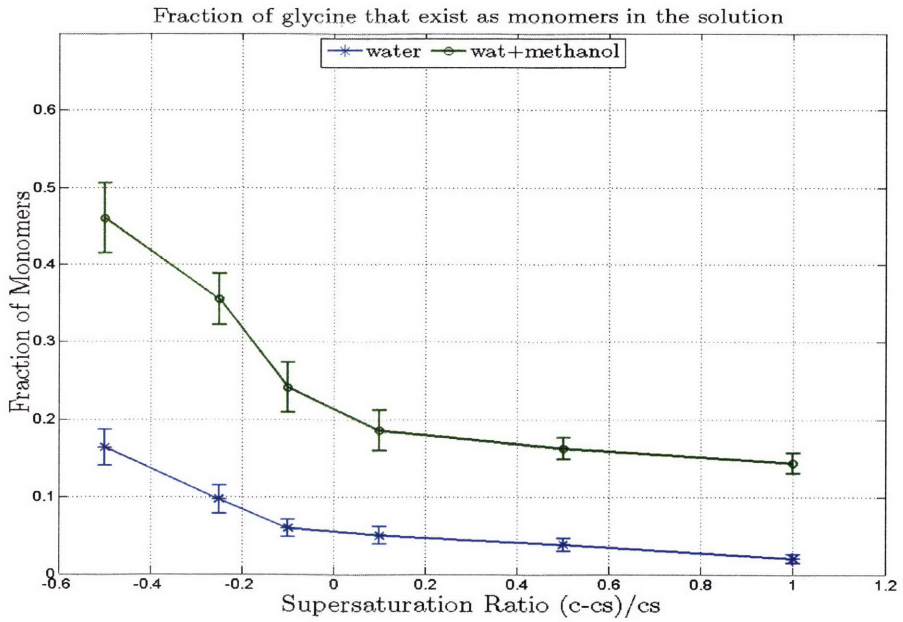


Figure 5-7: Fraction of glycine molecules that exist as monomers in water and water-methanol mixtures at various supersaturations.

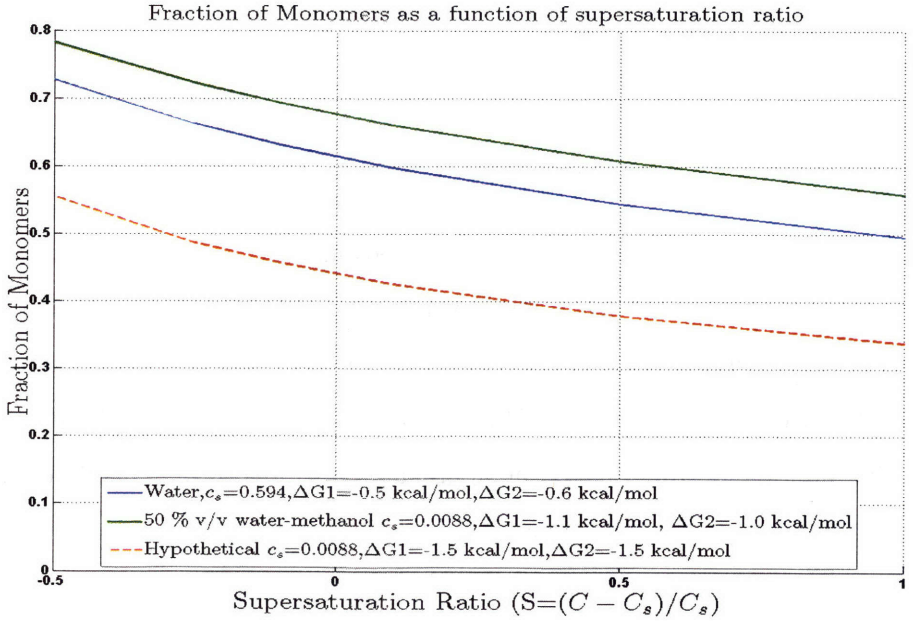


Figure 5-8: Predicted fraction of glycine monomers in water and water-methanol solvents and a hypothetical solvent at various supersaturations.

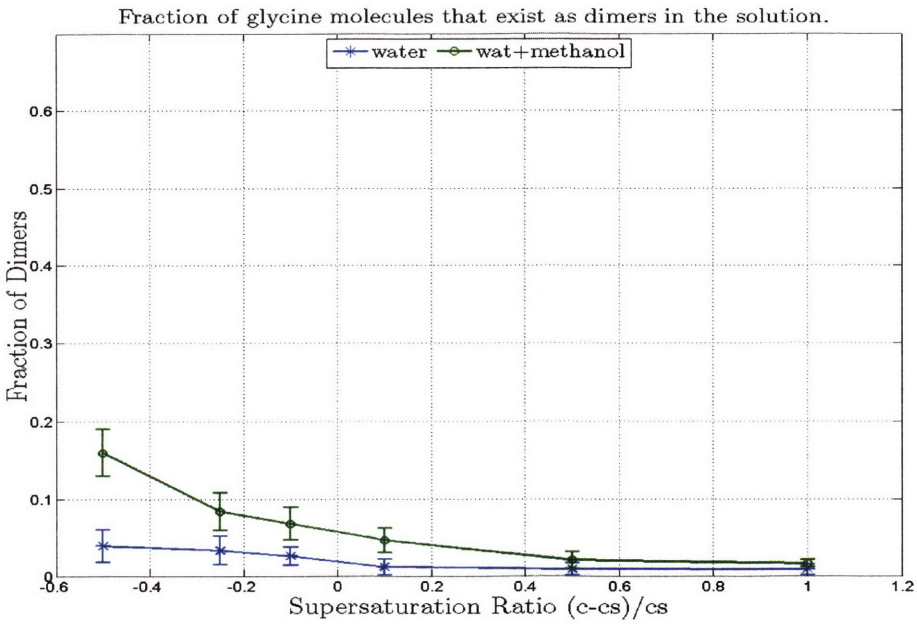


Figure 5-9: Fraction of glycine molecules that exist as dimers in the solution of water and water-methanol solvents.

## 5.3 Simulations of $\alpha$ & $\beta$ Glycine Interfaces

In this section MD Simulations of glycine crystal interfaces were performed to explore the solvent effect on crystal growth. Molecular dynamics and Free Energy calculations were performed in the previous section to understand the increase in glycine monomers in the presence of methanol additive. It was suggested that these monomers dock onto the (010) interface $\alpha$-glycine and further inhibit crystal growth. Simulations were carried out to explore the interface behavior of $\alpha$-glycine with and without monomer units at the interface. Various features like density, specific adsorption sites, energetics etc. are evaluated to obtain insights in the solvent effects on the crystal interface. The results are discussed in the following sections.

### 5.3.1 System Setup

The simulation cells consisted of $\alpha$ and $\beta$ glycine crystals with (010) and $(0\bar{1}0)$ faces exposed to water and water-methanol solutions.In the case of $\alpha$-glycine two cases

were considered, one with C—H bonds exposed and the other with N—H bonds exposed at the interface. Figures 5-10 and 5-11 show snapshots of the $\alpha$-glycine interfaces and the $\beta$-glycine interfaces are shown in Figure 5-12. Water is the solvent used when the interface consists of exposed C—H bonds in $\alpha$-glycine and water-methanol solution is used for exposed N—H bonds in $\alpha$-glycine and $\beta$-glycine. This is because $\beta$-glycine is only crystallized in water-methanol solutions and an interface with exposed N—H bonds in $\alpha$-glycine is only possible when methanol is added to water. The concentration of methanol is 0.3088 mole fraction (corresponding to 50% v/v water-methanol mixture).

Periodic boundary conditions were applied in all three dimensions. When simulating such interfaces it is important to have the thickness of the solvent layer to be at least four times the cutoff radius and the thickness of the crystal slab to be at least two times the cutoff radius to prevent any artifacts caused due to the use three dimensional periodic boundary conditions, such as interactions between water molecules at one crystal interface with the water molecules at the other face (across the crystal boundary). The cutoff radius used was 14 Å. The thickness of the crystal slab is 48 Å in $\alpha$-glycine (corresponding to $9X4X9$ crystal unit cells) and the thickness of the water layer is about 80 Å, both well within the constraints. The OPLS force field with modified $\alpha$-hydrogen parameters validated in the earlier section was used for glycine, and OPLS parameters were used for water and methanol. Ewald summation is used to calculate the electrostatic interactions for the system.

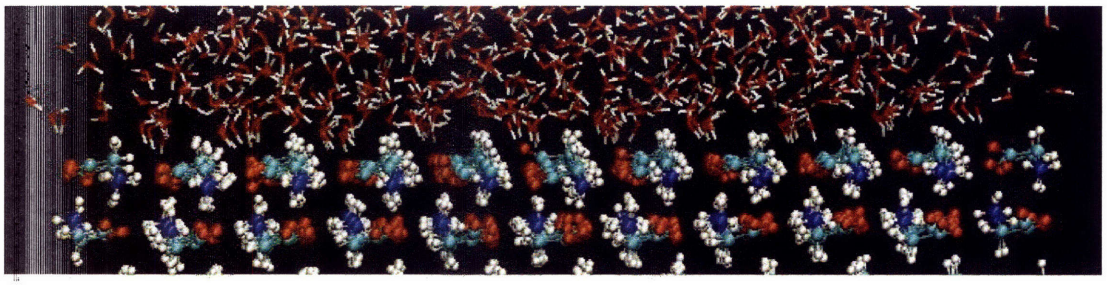

Figure 5-10: Schematic of the interface with water and (010) face of $\alpha$-glycine with C—H groups exposed.

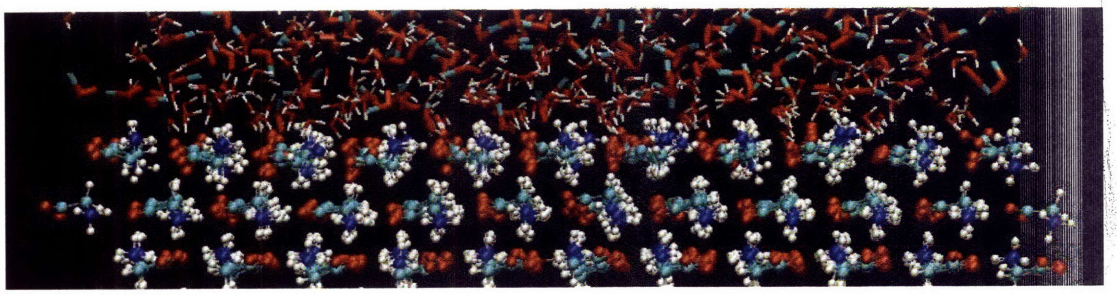

Figure 5-11: Schematic of the interface with water-methanol mixture and (010) face of $\alpha$-glycine with N—H groups exposed

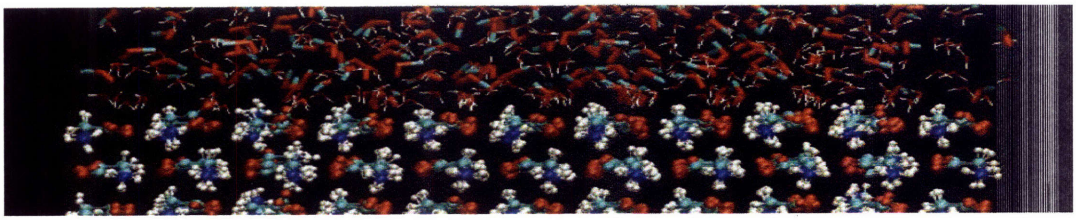

(a)

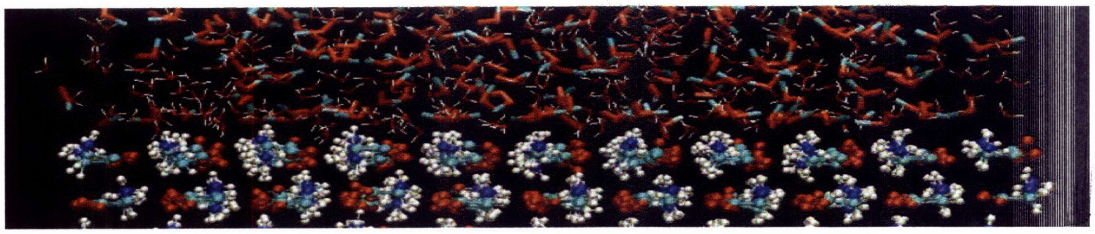

(b)

Figure 5-12: Schematic of the interface with water-methanol mixture and $(a)$ (010) and $(b)$ $(0\bar{1}0)$ of $\beta$-glycine.

### 5.3.2 Density Profiles

Comparing the density of the solvent on different interfaces provides qualitative description of the extent of solvent adsorption. For the calculation of density, the system is divided into bins of 0.25 Åperpendicular to the interface and the center of mass of solvent molecules is used. The center of mass of glycine molecules at the interface is used to define the crystal-solvent interface ($y = 0$). Density plots on both (010) and $(0\bar{1}0)$ interfaces are shown in the figures below. The peaks in the density profiles close to the interface indicate distinct surface layers present on the interface. Moving

away from the surfaces, the density becomes more uniform. The width of these peaks is used to define the structured layers of water. Figure 5-13 shows the density profiles of water on the (010) and $(0\bar{1}0)$ interfaces when the C—H groups are exposed (water is the only solvent). The density profiles are symmetrical due to the symmetry of the molecules in the unit cell at (010) and $(0\bar{1}0)$ faces.

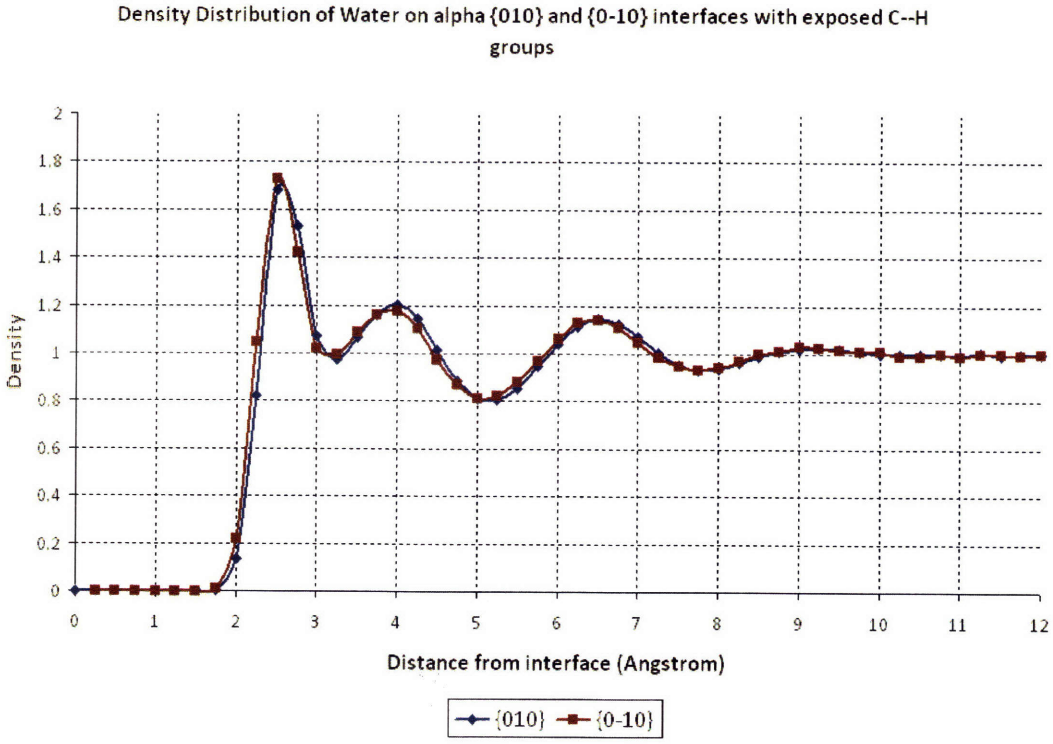


Figure 5-13: Density of water on (010) and $(0\bar{1}0)$ interfaces of $\alpha$-glycine with C—H groups exposed at the interface.

Figure 5-14 describes the density profiles of water on (010) and $(0\bar{1}0)$ interfaces when the N—H groups are exposed. As can be seen from the plots $(0\bar{1}0)$ has slightly higher water adsorption than the (010) interface. Similar plots for methanol are shown in Figure 5-15. Since we are interested in growth inhibition by the solvent on the faster growing interface, the (010) interface is used for analysis. Figure 5-16 shows the difference in water density profiles and the extent of adsorption when the C—H groups are exposed and when the N—H groups are exposed at the interface. It can be clearly observed that water penetration is more in the case of exposed N—H

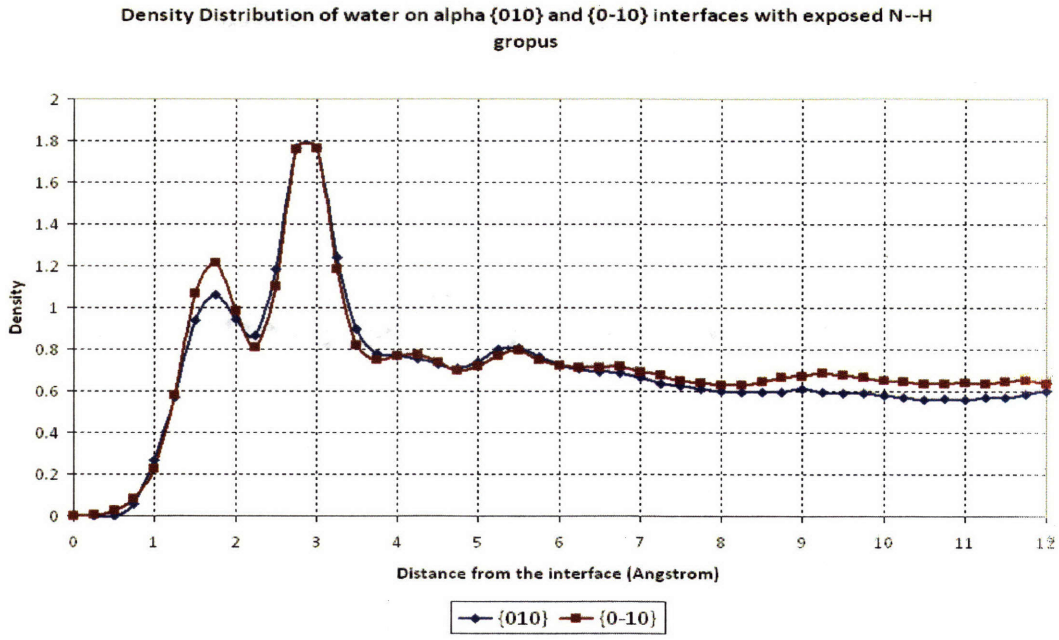


Figure 5-14: Density of water on (010) and $(0\bar{1}0)$ interfaces of $\alpha$-glycine with N—H groups exposed at the interface.

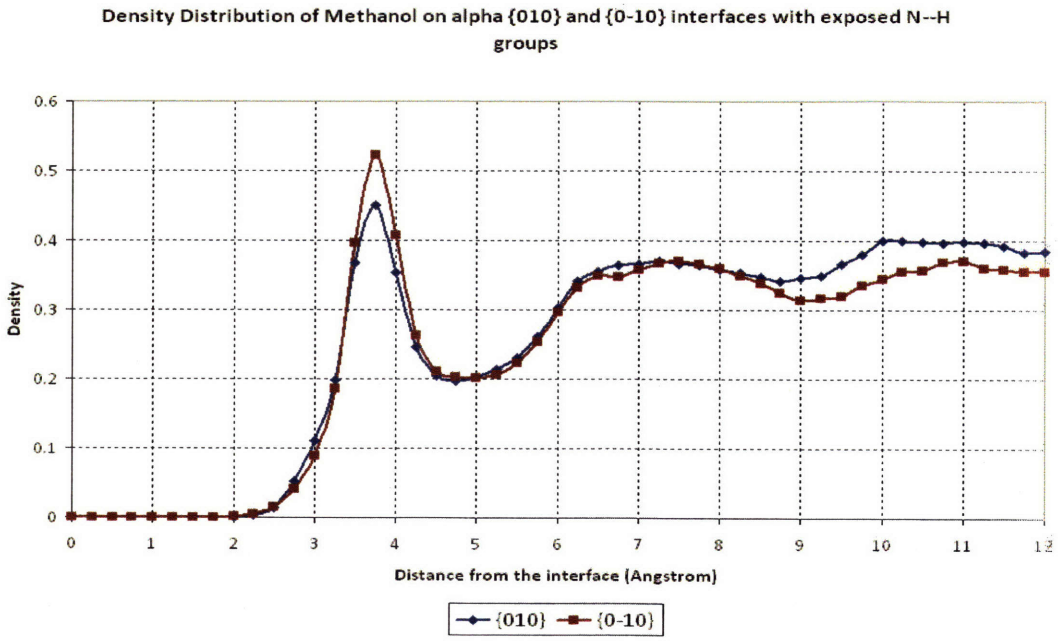


Figure 5-15: Density of methanol on (010) and $(0\bar{1}0)$ interfaces of $\alpha$-glycine with N—H groups exposed at the interface.

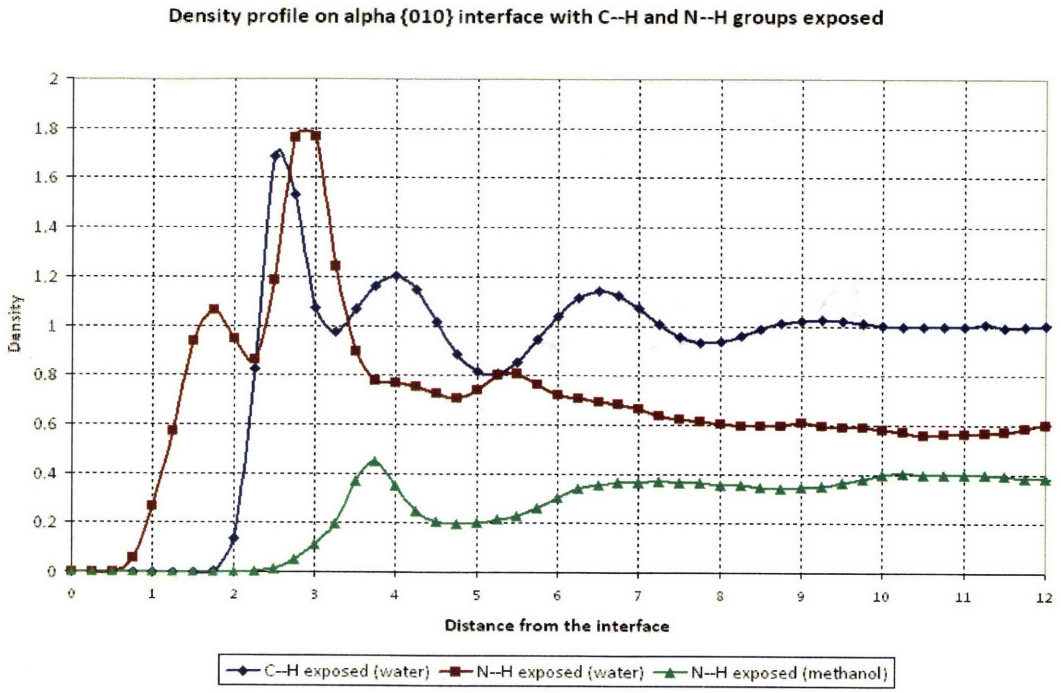


Figure 5-16: Density comparison of solvent molecules on (010) interface of $\alpha$-glycine with C—H and N—H groups exposed at the interface.

groups. In both cases two water layers are observed but the layers are closer to the interface with narrower widths in the case of exposed N—H groups implying more adsorption as predicted by the hypothesis. An important observation made possible through molecular dynamics is the behavior of methanol at the interface. There is only one peak of methanol observed which is present after the peak of second layer of water implying that water plays the major role in inhibiting growth.

Density plots for $\beta$-glycine interfaces are also plotted in Figures 5-17 and 5-18. As previously reported [4], the (010) interface of $\beta$-glycine grows at a slower rate than the (010) face. Although the (010) face is very similar to (010) face of $\alpha$-glycine with C—H groups exposed and the $(0\bar{1}0)$ face is very similar to (010) face of $\alpha$-glycine with N—H groups exposed, the density profiles look different. In the case of $\beta$-glycine both water and methanol solvents show varying density profiles at (010) and $(0\bar{1}0)$ interfaces and hence both the solvents play a role in inhibiting crystal growth.

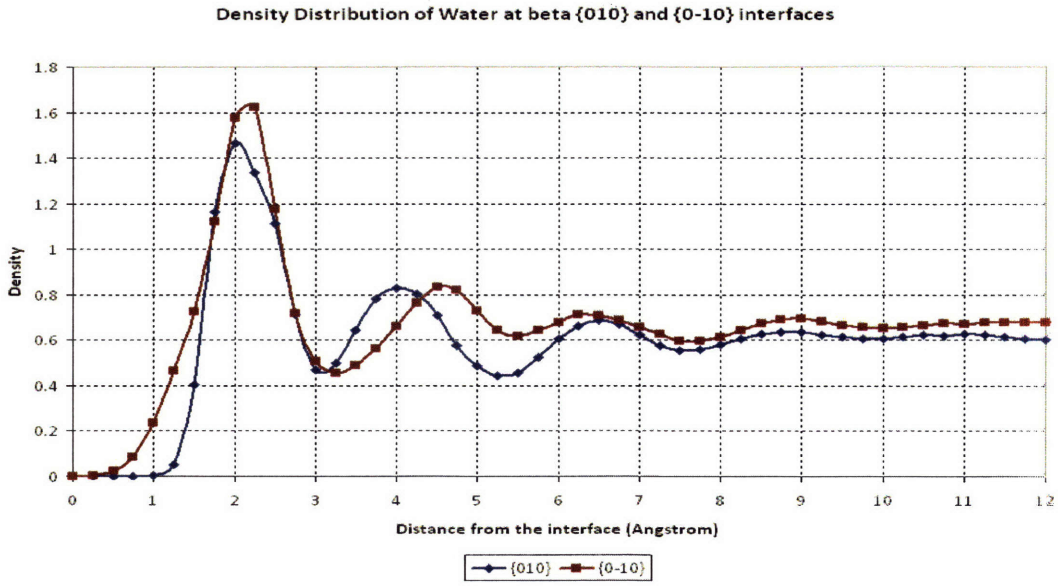


Figure 5-17: Density of water on (010) and $(0\bar{1}0)$ interfaces of $\beta$-glycine.

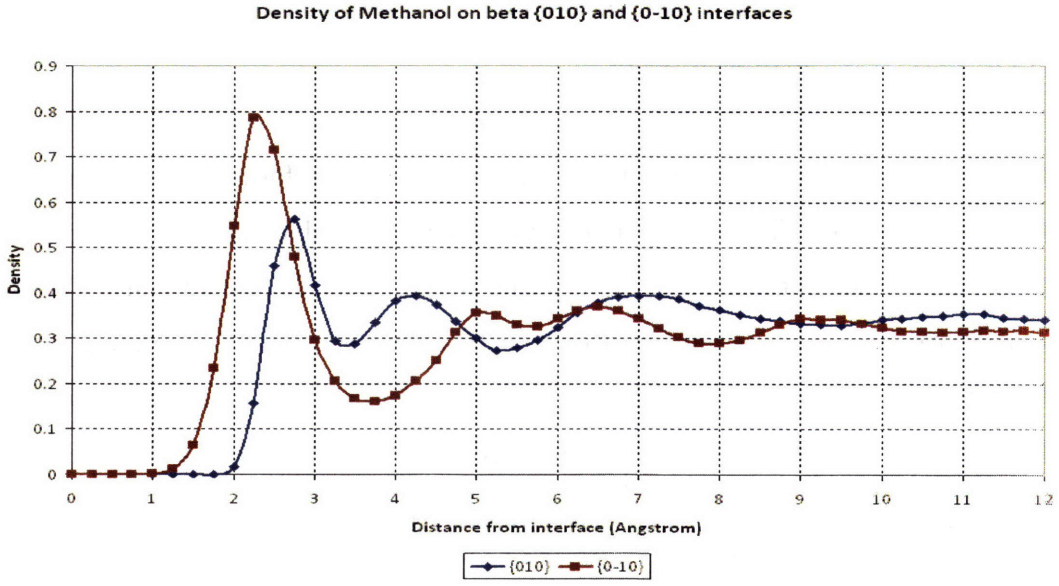


Figure 5-18: Density of methanol on (010) and $(0\bar{1}0)$ interfaces of $\alpha$-glycine

### 5.3.3 Scatter Plots & Energetics

To obtain a quantitative picture of the structured layers close to the interface with C—H and N—H groups exposed, the center of mass motion of solvent molecules is explored for 50 picoseconds during the simulation. This is done by plotting the

trajectories of center of mass of solvent molecules in the layers defined by the density plots. The widths of the first two peaks are used and the scatter plots were plotted for the two layers with water and water-methanol solvents.

Figure 5-21 and Figure 5-22 show the scatter plot of solvent in the first structured layer. As can be observed the first layer for water-methanol solvent is less populated but more concentrated at specific sites on the interface. The first layer for water solvent also exhibits preferential absorption on specific sites although the order is less compared to the case with water-methanol solvent. These adsorption sites on the interfaces with C—H bonds and N—H bonds exposed are identified from the snapshots of these layers taken from the simulations. Figure 5-19 illustrates the structured layer observed at the interface with C—H bonds exposed. The water molecules form strong $H_{water} \cdots COO^-$ hydrogen bonds and weak $O_{water} \cdots CH$ hydrogen bonds. Similar observations are made for the structured water layer on the interface with N—H bonds exposed (Figure 5-20). The water molecules in this case form strong $H_{water} \cdots COO^-$ and $O_{water} \cdots NH^+$ hydrogen bonds.

These specific islands of adsorption are further studied through interaction energy calculations. Energetic calculations similar to the ones performed by Anwar et al. [71] were performed. The interaction energy specified in Table 5.3 is the electrostatic and Lennard-Jones interactions between one water molecule and the entire crystal averaged over time. This energy is used to categorize the strength of binding for the solvent molecules on the interface. An increase in interaction energy of about 36.2 KJ/mol is observed when the N—H bonds are exposed at the interface.

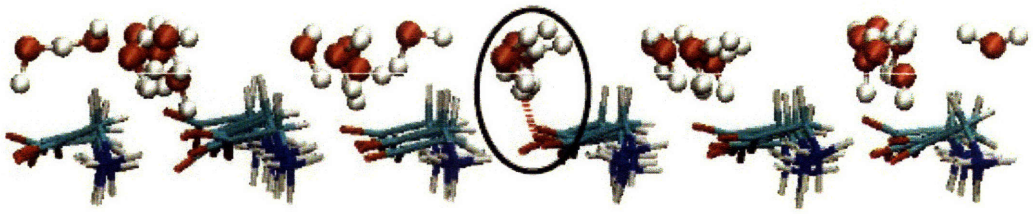

Figure 5-19: Snapshot of the first structured layer on $\alpha$-glycine interface with C—H groups exposed.

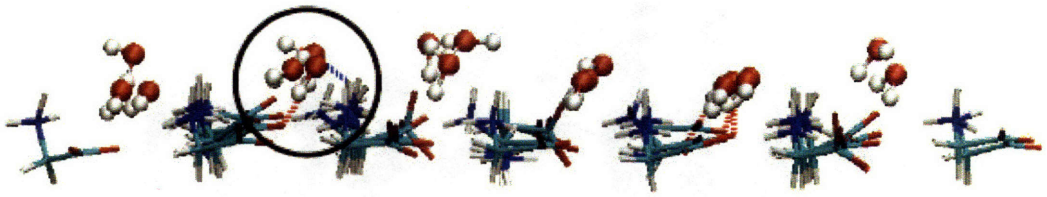

Figure 5-20: Snapshot of the first structured layer on $\alpha$-glycine interface with N—H groups exposed.

Table 5.3: Interaction Energy of water at the specific sites with the $\alpha$-glycine interface

| Interface | Interaction Energy at specific sites (KJ/mol) |
|---|---|
| (010) $\alpha$-glycine with C—H bonds exposed | -33.7 |
| (010) $\alpha$-glycine with N—H bonds exposed | -69.4 |

Similar observations are made for the second layer with water and water-methanol solvents (Figures 5-23 and 5-24), there is no preferential adsorption in the second layer but the order is greatly reduced when the C—H groups are exposed at the interface. This is a clear indication of increased interactions for the solvent with N—H groups than with the C—H groups.

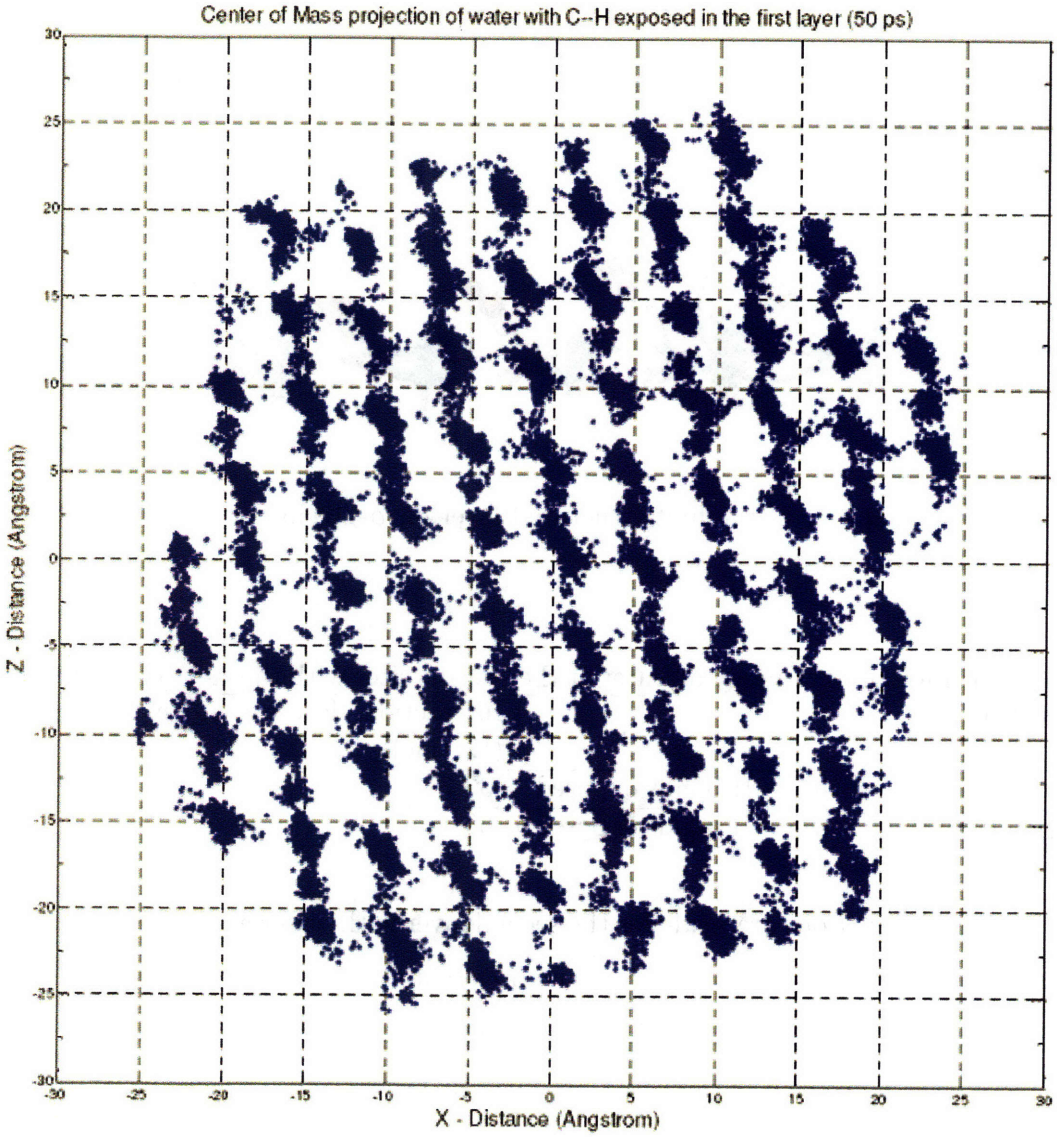


Figure 5-21: Center of Mass distribution of water molecules on the $\alpha$-glycine interface with C—H groups exposed in the first structured layer.

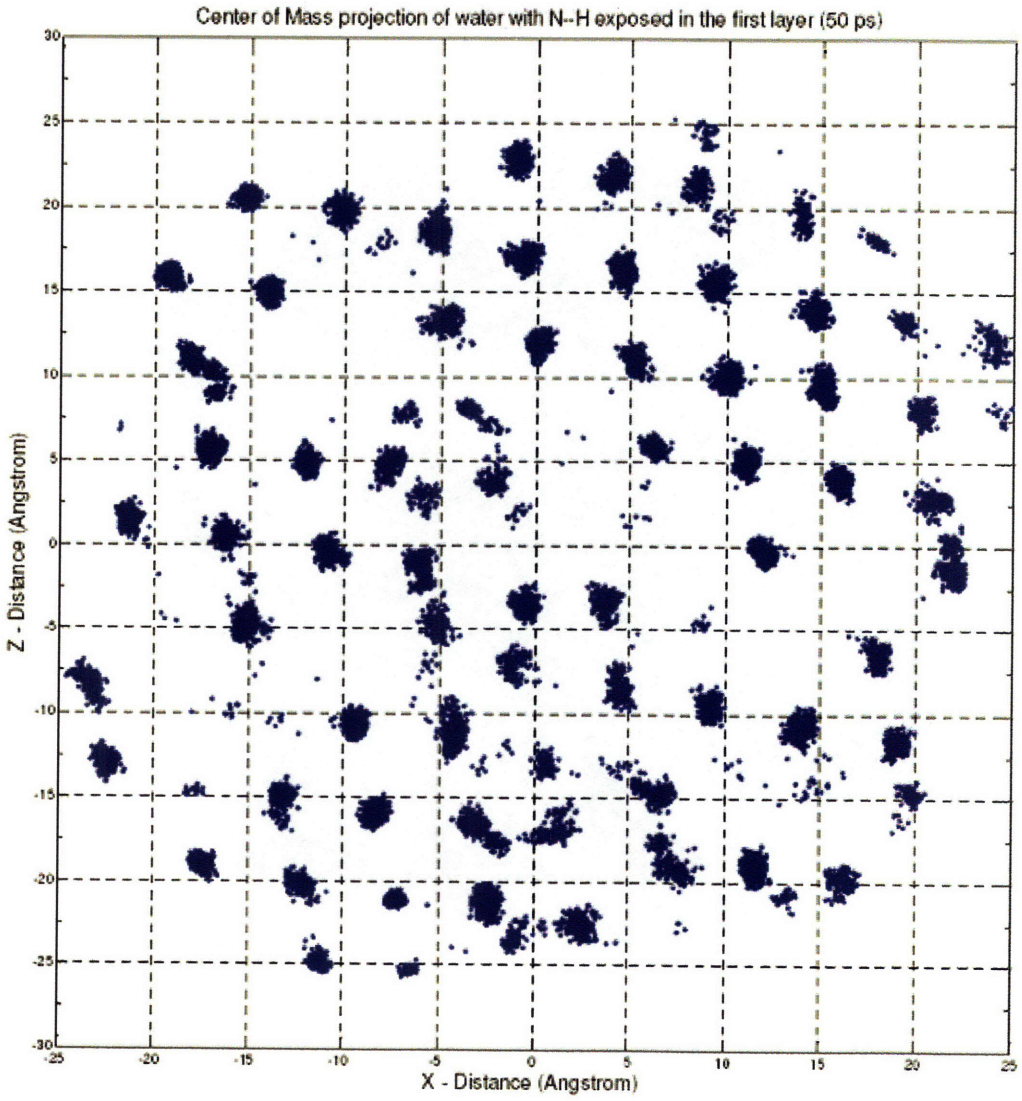


Figure 5-22: Center of Mass distribution of water molecules on the $\alpha$-glycine interface with N—H groups exposed in the first structured layer.

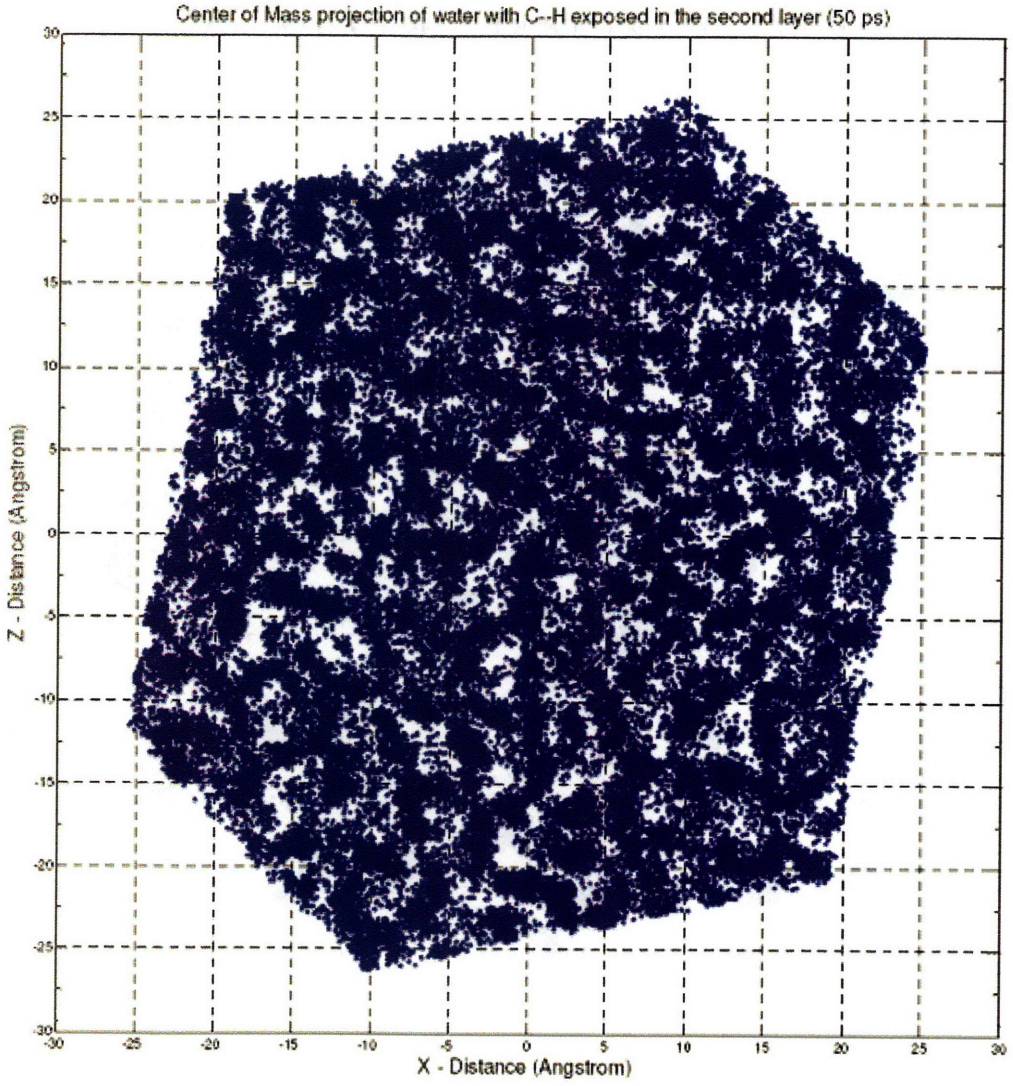


Figure 5-23: Center of Mass distribution of water molecules on the $\alpha$-glycine interface with C—H groups exposed in the second structured layer.

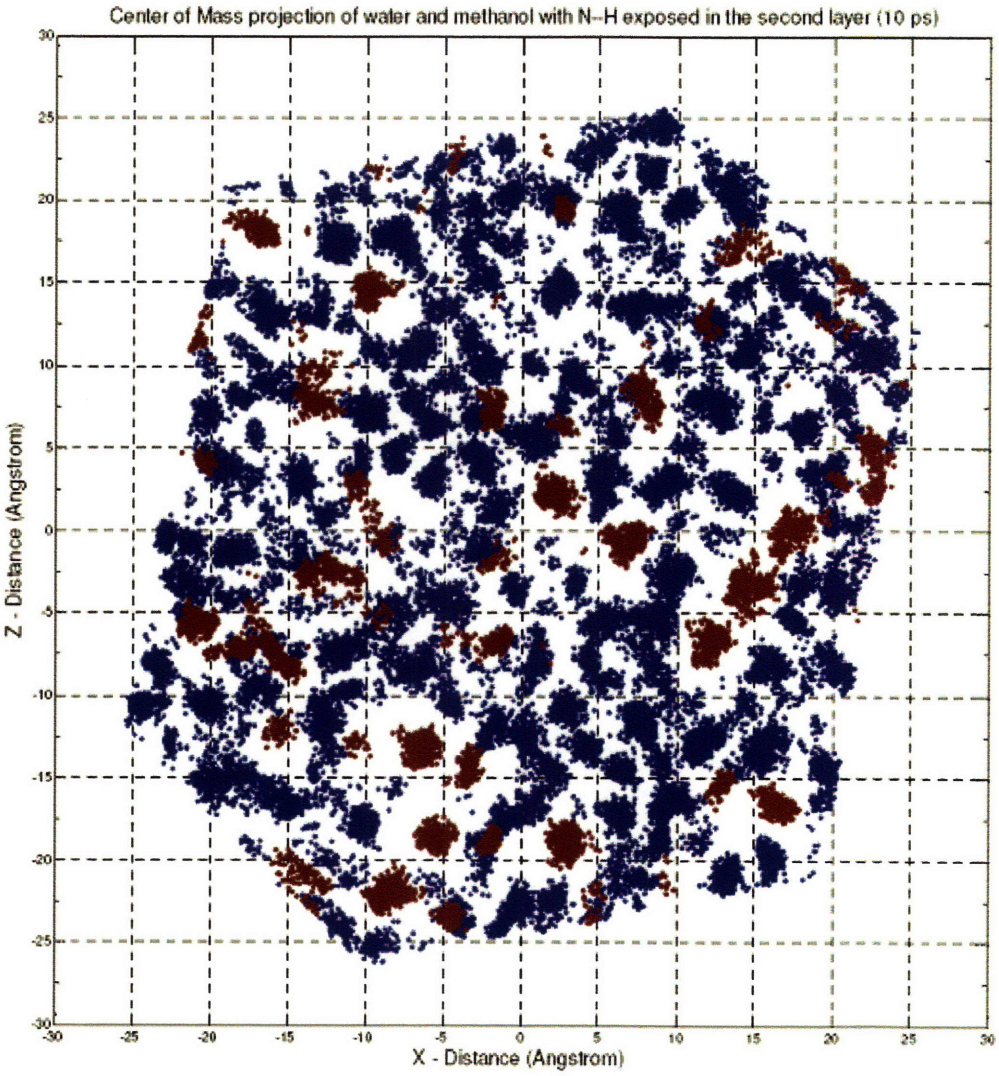


Figure 5-24: Center of Mass distribution of water and methanol molecules on the $\alpha$-glycine interface with N—H groups exposed in the second structured layer.

# Chapter 6

# Conclusions & Future Work

The force fields and parameters available in literature have been tested for their ability to simulate all the glycine polymorphs. AMBER failed to reproduce the $\alpha$ and $\beta$ glycine structures and CHARMM failed in simulating $\alpha$ and $\gamma$ glycine. The OPLS force field and parameters were successful in maintaining the hydrogen bond networks of glycine polymorphs but showed large deviations in lattice parameters. Better agreement with experimental observations was obtained by slightly modifying the Lennard-Jones parameters of the hydrogen atoms attached to the $\alpha$-carbon. The Lennard Jones parameters for this hydrogen atom were adapted from AMBER parameters for glycine zwitterion. These parameters showed considerable improvement both in lattice parameters and hydrogen network stability. The parameters were further tested for stability in molecular dynamics. Constant pressure (1 atm) and temperature (300 K) simulations of the polymorphs for one nanosecond with triclinic boundary conditions were performed. The lattice parameters were found to be stable and within reasonable limits of the experimental values. The force field and parameters were also successfully vailidated for their ability to model solution behavior in water by comparing coordination numbers with experimental observations.

The solution behavior of glycine has been studied to investigate the reasons behind crystallization of $\beta$-glycine in water-methanol mixtures. Weissbuch et al. [4] postulated an increase in the glycine monomer units in the presence of the methanol additive, but the reason was unclear. Free energy calculations for the dimerization

reaction were performed with and without a methanol additive. The reactant state corresponds to two glycine monomers. The product state is the double hydrogen bonded dimer unit. The free energy difference and the activation barrier for the reaction (Figure 5-4) indicate higher stability of the centrosymmetric dimer unit in 50% v/v water-methanol mixtures. Glycine dimer with one hydrogen bond was found to be an intermediate state. Solutions of glycine in water and water-methanol mixtures were simulated over various supersaturations and the fraction of monomers and dimers were calculated. Over the supersaturation levels explored a higher fraction of monomers was observed in water-methanol mixtures. The higher fraction of monomers was interpreted using simple mass action laws and equilibrium thermodynamics. It was concluded that at similar supersaturation levels solubility and dimer stability play opposing roles in governing the monomer fraction in solutions and the drastic decrease in solubility due to the presence of methanol additive results in an increased fraction of monomers.

The nuclei of $\alpha$-glycine type that are formed in the solutions are inhibited at the crystal growth stage. An increase in glycine monomer units will result in the formation of interfaces, with N—H bonds exposed on the $\alpha$-glycine interface. The ability of solvent to inhibit the crystal growth at these interfaces is explored through simulations of $\alpha$-glycine interfaces with both C—H and N—H bonds exposed. The density profiles, scatter plots, and energetics of interactions on the interface clearly indicate higher adsorption of the solvent at the interface with exposed N—H bonds. This would result in an increase in the barrier, $\Delta G_{deh}$ (Figure 2-4), for stripping the solvent molecules from the interface and hence an inhibition of crystal growth. The density profiles clearly indicate that water plays a dominating role in inhibiting crystal growth when growth occurs through docking of monomer (010) crystal interface which expose N—H groups to the solvent.

It is concluded that the role of the methanol additive is to increase the percentage of glycine monomer units in the solution. Methanol being less polar than water has a much lower solubility of glycine. The stability of $\alpha$-glycine growth unit increases in 50% v/v water-methanol mixtures. If only the growth synthon hypothesis were to be

considered, $\alpha$-glycine would be predicted in water-alcohol solutions. Link hypothesis postulates that the most stable growth unit in the solution would present itself in the final crystal structure. We conclude that both the stability of the growth synthon and the supersaturation play important roles in determining the final polymorph outcome, and in this case the effect of supersaturation dominates the stability of the $\alpha$-glycine growth synthon, resulting in the growth inhibition of $\alpha$-glycine polymorph.

The interface simulations of $\gamma$-glycine proved challenging due to the difficulty of simulating a polar crystal interface. The $\gamma$-glycine crystal has a net dipole moment perpendicular to the $\{001\}$ interface. Simulations of such interfaces have been carried out in the literature but are limited to ionic crystals. Development of a method to simulate polar interfaces in organic crystals would lead to key insights on the 'relay growth' mechanism.

In summary, key qualitative insights into the methanol additive effect on polymorph selection during glycine crystallization were obtained through molecular dynamics simulations of solution behavior of glycine. But in order to obtain any quantitative results that would form the basis for a rational algorithm for the screening of solvents, it is absolutely necessary to understand the nucleation mechanism and also the structure of the critical nucleus. Future studies in this direction would facilitate in the determination of rate equations and in isolation of the key properties of the solvent that effect the polymorphic outcome.

# Bibliography


[1] Lian Yu, G. A. Stephenson, C. A. Mitchell, C. A. Bunnell, S. V. Snorek, J. J. Bowyer, T. B. Borchardt, and J. G. Stowell adn S. R. Byrn. Thermochemistry and conformational polymorphism of a hexamorphic crystal system. *J. Am. Chem. Soc.*, 122(4):585–591, 2000.

[2] R. J. Davey, K. Allen, N. Blagden, W. I. Cross, H. F. Liebermann, M. J. Quayle, S. Righini, L. Seton, and G. J. T. Tiddy. Crystal engineering - nucleation, the key step. *CrystEngComm*, 4(47):257–264, 2002.

[3] P. Bennema. Analysis of crystal growth models for slightly supersaturated solutions. *Journal of Crystal Growth*, 1:278–286, 1967.

[4] I. Weissbuch, V. Yu. Torbeev, L. Leiserowitz, and M. Lahav. Solvent effect on crystal polymorphism: Why addition of methanol or ethanol to aqueous solutions induces the precipitation of the least stable $\beta$ form of glycine. *J. Am. Chem. Soc.*, 110:7690–7697, 2001.

[5] I. Weissbuch, L. Addai, and L. Leiserowitz. Molecular Recognition at Crystal Interfaces. *Science*, 253(5020):637–645, 1991.

[6] J. Kottalam and D. A. Case. Dynamics of ligand escape from the heme pocket of myoglobin. *J. Am. Chem. Soc.*, 110:7690–7697, 1988.

[7] J. W. Mullin. *Crystallization*. Butterworth-Heinemann, fourth edition, 9 May 2001.

[8] H.N. de Armas, O.M. Peeters, N. Blaton, D.J.A. De Ridder, and H. Schenk. X-ray powder diffraction data and crystal data of polymorphic form 2 of carnidazole. *Powder Diffraction*, 21:56, 2006.

[9] J. Bauer, S. Spanton, R. Henry, J. Quick, W. Dziki, W. Porter, and J. Morris. Ritonavir: An extraordinary example of conformational polymorphism. *Pharmaceutical Research*, 18(6):859–866, 2001.

[10] T. L. Threlfall. Analysis of organic polymorphs. a review. *The Analyst*, 120(10):2435, 1995.

[11] H. Ando, M. Ishii, M. Kayano, and H. Ozawa. Effect of moisture on crystallization of theophylline in tablets. *Drug Development and Industrial pharamacy*, 18(4):453–467, 1992.

[12] K. R. Morris, A. W. Newman, D. E. Bugay, S. A. Ranadive, A. K. Singh, M. Szyper and. S. A. Varia, H. G. Brittain, and T. M. Serajuddin. Characterization of humidity-dependent changes in crystal properties of a new hmg-coa reductase inhibitor in support of its dosage form development. *International Journal of Pharmaceutics*, 108(3):195–206, 1994.

[13] M. Otsuka and Y. Matsuda. Effects of environmental temperature and compression energy on polymorphic transformation during tabletting: Pharmaceutical compaction Research Laboratory and Information Center. Annual symposium. *Drug development and industrial pharmacy*, 19(17-18):2241–2269, 1993.

[14] I. Weissbuch, M. Lahav, and L. Leiserowitz. Toward stereochemical control, monitoring, and understanding of crystal nucleation. *Crystal growth & design*, 3(2):125–150, 2003.

[15] FJJ Leusen. Ab initio prediction of polymorphs. *Journal of Crystal Growth*, 166(1):900–903, 1996.

[16] A. Gavezzotti, G. Filippini, J. Kroon, BP Van Eijck, and P. Klewinghaus. The Crystal Polymorphism of Tetrolic Acid (CH 3 CCCOOH): A Molecular Dynamics study in solution, and a Crystal Structure Generation. *Chemistry(Weinheim)*, 3(6):893–899, 1997.

[17] EB Treivus. Solvent effect on the kinetics of crystal growth. *Russian Chemical Reviews*, 61(7):673–682, 1992.

[18] RJ Davey. The Role of the Solvent in Crystal Growth from Solution. *J. Crystal Growth*, 76:637–644, 1986.

[19] A. C. Zettlemoyer. *Nucleation Phenomena.* Marcel Dekker, 1969.

[20] W. Ostwald. *Z. Phys. Chem.*, 22:289, 1897.

[21] G. Nichols and C.S. Frampton. Physicochemical characterization of the orthorhombic polymorph of paracetamol crystallized from solution. *Journal of Pharmaceutical Sciences*, 87(6):684–693, 1998.

[22] Becker D. and Döring W. The kinetic treatment of nuclear formation in supersaturated vapors. *Annalen der Physik*, 24:719–752, 1935.

[23] M. Volmer and A. Weber. Keimbildung in übersättigten gebilden. *Z. Phys. Chem.*, page 227, 1925.

[24] M. Volmer. Kinetik den Phasenbildung. Leipzig, Dresden: Th. Steinkopf, 1939. Vgl. hicrzu: a) Vetter, KJ: Electrochemical Kinetics, 1967.

[25] D. Turnbull and JC Fisher. Rate of Nucleation in Condensed Systems. *The Journal of Chemical Physics*, 17:71, 2004.

[26] D.W. Oxtoby and R. Evans. Nonclassical nucleation theory for the gas–liquid transition. *The Journal of Chemical Physics*, 89:7521, 1988.

[27] D.W. Oxtoby. Nucleation of first-order phase transitions. *Acc. Chem. Res*, 31(1):91, 1998.

[28] J.P. Behr. *The Lock-and-key Principle: The State of the Art–100 Years on*, page 173. Wiley, 1994.

[29] A. Gavezzotti and G. Filippini. Self-organization of small organic molecules in liquids, solutions and crystals: static and dynamic calculations. *Chemical Communications*, 1998(3):287–294, 1998.

[30] PR ten Wolde and D. Frenkel. Enhancement of protein crystal nucleation by critical density fluctuations. *Science*, 277(5334):1975–8, 1997.

[31] J. Anwar and P.K. Boateng. Computer Simulation of Crystallization from Solution. *Springer Ser. Chem. Phys*, page 43, 1987.

[32] J.D. Shore, D. Perchak, and Y. Shnidman. Simulations of the nucleation of AgBr from solution. *The Journal of Chemical Physics*, 113:6276, 2000.

[33] S. Chattopadhyay, D. Erdemir, J.M.B. Evans, J. Ilavsky, H. Amenitsch, C.U. Segre, and A.S. Myerson. SAXS study of the nucleation of glycine crystals from a supersaturated solution. *Crystal Growth & Design*, 5(2):523–527, 2005.

[34] R. Radhakrishnan and B.L. Trout. Nucleation of Hexagonal Ice (I h) in Liquid Water. *J. AM. CHEM. SOC*, 125:7743, 2003.

[35] J.M. Leyssale, J. Delhommelle, and C. Millot. Atomistic simulation of the homogeneous nucleation and of the growth of N crystallites. *The Journal of Chemical Physics*, 122:104510, 2005.

[36] J.M. Leyssale, J. Delhommelle, and C. Millot. Molecular simulation of the homogeneous crystal nucleation of carbon dioxide. *The Journal of Chemical Physics*, 122:184518, 2005.

[37] S. Parveen, RJ Davey, G. Dent, and RG Pritchard. Linking solution chemistry to crystal nucleation: the case of tetrolic acid. *Chemical Communications*, 2005(12):1531–1533, 2005.

[38] L.R. MacGillivray and M.J. Zaworotko. Crystal and molecular structure of 2, 6-dihydroxybenzoic acid. *Journal of Chemical Crystallography*, 24(10):703–705, 1994.

[39] M. Gdaniec, M. Gilski, and GS Denisov. $\gamma$-Resorcyclic acid, its monohydrate and its pyridinium complex. *Acta crystallographica. Section C, Crystal structure communications*, 50:1622–1626, 1994.

[40] RJ Davey, N. Blagden, S. Righini, H. Alison, MJ Quayle, and S. Fuller. Crystal Polymorphism as a Probe for Molecular Self-Assembly during Nucleation from Solutions: The Case of 2, 6-Dihydroxybenzoic Acid. *Crystal Growth & Design*, 1(1):59–65, 2001.

[41] R.J. Davey, W. Liu, M.J. Quayle, and G.J.T. Tiddy. In Situ Monitoring of Crystallization Processes Using Synchrotron X-ray Diffraction: The Search for Structural Precursors. *Crystal Growth & Design*, 2(4):269–272, 2002.

[42] RJ Davey, G. Dent, RK Mughal, and S. Parveen. Concerning the Relationship between Structural and Growth Synthons in Crystal Nucleation: Solution and Crystal Chemistry of Carboxylic Acids As Revealed through IR Spectroscopy. *Crystal Growth & Design*, 6(8):1788–1796, 2006.

[43] A. F. Wells. *New Investigations in Crystallography and Crystal Chemistry: Translated into Russian*, volume 5. Izdatinlit, Moscow, second edition, 1950.

[44] D. H. Watson. In V. E. Cosslett, editor, *Proc. of the Third International Conference on Electron Microscopy*, page 497, London, 1954. Royal Microscopical Society.

[45] W. Kleber and H. Raidt. *Z. Phys. Chem.*, 222, 1963.

[46] R. J. Davey. *Current Topics in Materials Science*, volume 8, chapter 6. North Holland, Amsterdam, 1982.

[47] P. Bennema and G. Gilmer. *Crystal Growth: An Introduction*, chapter 10. North Holland, Amsterdam, 1973.

[48] WK Burton, N. Cabrera, and FC Frank. The Growth of Crystals and the Equilibrium Structure of their Surfaces. *Philosophical Transactions of the Royal Society of London. Series A, Mathematical and Physical Sciences*, 243(866):299–358, 1951.

[49] LJW Shimon, M. Vaida, L. Addadi, M. Lahav, and L. Leiserowitz. Molecular recognition at the solid-solution interface: a relay mechanism for the effect of solvent on crystal growth and dissolution. *Journal of the American Chemical Society*, 112(17):6215–6220, 1990.

[50] LJW Shimon, FC Wireko, J. Wolf, I. Weissbuch, L. Addadi, Z. Berkovitch-yeelin, M. Lahav, and L. Leiserowitz. Assignment of Absolute Structure of Polar Crystals Using Tailor-Made Additives. Solvent Surface Interactions on the Polar Crystals of $\alpha$-Resorcinol,(R, S) Alanine and Y-Glycine. *Molecular Crystals and Liquid Crystals*, 137(1):67–86, 1986.

[51] LJW Shimon, M. Lahav, and L. Leiserowitz. Design of stereoselective etchants for organic crystals. Application for the sorting of enantiomorphs and direct assignment of absolute configuration of chiral molecules. *Journal of the American Chemical Society*, 107(11):3375–3377, 1985.

[52] E.V. Boldyreva, V.A. Drebushchak, T.N. Drebushchak, I.E. Paukov, Y.A. Kovalevskaya, and E.S. Shutova. Polymorphism of glycine: Thermodynamic aspects. Part I. Relative stability of the polymorphs. *Journal of Thermal Analysis and Calorimetry*, 73(2):409–418, 2003.

[53] D. Bernal. *Z. Krist.*, 78:363, 1931.

[54] J. Hengstenberg and F. V. Lenel. *Z. Krist.*, 77:424, 1931.

[55] G. Albrecht and RB Corey. The crystal structure analysis of glycine. *J. Amer. Chem. Soc*, 61:1087–1103, 1939.

[56] RE Marsh. A refinement of the crystal structure of glycine. *Acta Crystallographica*, 11(9):654–663, 1958.

[57] Fischer E. *Ber. Deut. Chem. Ges.*, 38:2917, 1904.

[58] Y. Iitaka. The crystal structure of $\beta$-glycine. *Acta Crystallographica*, 13(1):35–45, 1960.

[59] Y. Iitaka. In *Proc. of the Japan Academy*, page 109, 1954.

[60] Y. Iitaka. The crystal structure of $\gamma$-glycine. *Acta Crystallographica*, 11(3):225–226, 1958.

[61] Y. Iitaka. The Crystal Structure of $\gamma$-Glycine. *Acta Cryst*, 14:1, 1961.

[62] Å. Kvick, WM Canning, TF Koetzle, and GJB Williams. An experimental study of the influence of temperature on a hydrogen-bonded system: the crystal structure of $\gamma$-glycine at 83 K and 298 K by neutron diffraction. *Structural Crystallography and Crystal Chemistry*, 36(1):115–120, 1980.

[63] WCM Lewis. The Crystallization, Denaturation and Flocculation of Proteins with Special Reference to Albumin and Hemoglobin; together with an Appendix on the Physicochemical Behavior of Glycine. *Chemical Reviews*, 8(1):81–165, 1931.

[64] D. Gidalevitz, R. Feidenhans'l, S. Matlis, D.M. Smilgies, MJ Christensen, and L. Leiserowitz. MONITORING IN SITU GROWTH AND DISSOLUTION OF MOLECULAR CRYSTALS: TOWARDS DETERMINATION OF THE GROWTH UNITS. *Angewandte Chemie. International edition in English*, 36(9):955–959, 1997.

[65] AS Myerson and P.I. Lo. Cluster formation and diffusion in supersaturated binary and ternary amino acid solutions. *Journal of crystal growth*, 110(1-2):26–33, 1991.

[66] J. W. Chew, S. N. Black, P. S. Chow, R. B. Tan, and K. J. Carpenter. Stable polymorphs: difficult to make and difficult to predict. *CrystEnggComm*, 9(2):128–130, 2007.

[67] C.S. Towler, R.J. Davey, R.W. Lancaster, and C.J. Price. Impact of Molecular Speciation on Crystal Nucleation in Polymorphic Systems: The Conundrum of Glycine and Molecular'Self Poisoning'. *Journal of the American Chemical Society*, 126(41):13347–13353, 2004.

[68] Z. Berkovitch-Yellin, L. Addadi, M. Idelson, L. Leiserowitz, and M. Lahav. Absolute configuration of chiral polar crystals. *Nature*, 296(5852):27–34, 1982.

[69] FC Wireko, LJW Shimon, F. Frolow, Z. Berkovitch-Yellin, M. Lahav, and L. Leiserowitz. Effect of solvent on the growth of organic crystals. 1. The riddle of. alpha.-resorcinol. *The Journal of Physical Chemistry*, 91(2):472–481, 1987.

[70] J.L. Wang, L. Leiserowitz, and M. Lahav. A correlation between surface wettability and solvent effect on crystal growth. The Nn-octyl-D-gluconamide/methanol system. *The Journal of Physical Chemistry*, 96(1):15–16, 1992.

[71] M. Hussain and J. Anwar. The Riddle of Resorcinol Crystal Growth Revisited: Molecular Dynamics Simulations of R-Resorcinol Crystal-Water Interface. *J. Am. Chem. Soc*, 121(37):8583–8591, 1999.

[72] I. Weissbuch, L. Leisorowitz, and M. Lahav. Tailor-made and charge-transfer auxiliaries for the control of the crystal polymorphism of glycine. *Advanced materials(Weinheim)*, 6(12):952–956, 1994.

[73] P.W. Carter, A.C. Hillier, and MD Ward. Nanoscale Surface Topography and Growth of Molecular Crystals: The Role of Anisotropic Intermolecular Bonding. *Journal of the American Chemical Society*, 116(3):944–953, 1994.

[74] F.H. Allen. The Cambridge Structural Database: a quarter of a million crystal structures and rising. *logo*, 58(1 Part 3):380–388.

[75] J.C. Phillips, R. Braun, W. Wang, J. Gumbart, E. Tajkhorshid, E. Villa, C. Chipot, R.D. Skeel, L. Kale, and K. Schulten. Scalable molecular dynamics with NAMD. *J. Comput. Chem*, 26(16):1781–1802, 2005.

[76] BR Brooks, RE Bruccoleri, BD Olafson, DJ States, S. Swaminathan, and M. Karplus. CHARMM: a program for macromolecular energy, minimization, and dynamics calculations. *Journal of computational chemistry*, 4(2):187–217, 1983.

[77] WL Jorgensen and J. Tirado-Rives. The OPLS potential functions for proteins. Energy minimizations for crystals of cyclic peptides and crambin. *Journal of the American Chemical Society*, 110(6):1657–1666, 1988.

[78] Y. Duan, C. Wu, S. Chowdhury, M.C. Lee, G. Xiong, W. Zhang, R. Yang, P. Cieplak, R. Luo, T. Lee, et al. A point-charge force field for molecular mechanics simulations of proteins based on condensed-phase quantum mechanical calculations. *Journal of Computational Chemistry*, 24(16):1999–2012, 2003.

[79] PP Ewald. Evaluation of optical and electrostatic lattice potentials. *Ann. Phys*, 64:253, 1921.

[80] D.L. Veenstra, D.M. Ferguson, and P.A. Kollman. How transferable are hydrogen parameters in molecular mechanics calculations? *Journal of Computational Chemistry*, 13(8):971–978, 1992.

[81] CM Freeman, JW Andzelm, CS Ewig, J.R. Hill, and B. Delley. The structure and energetics of glycine polymorphs based on first principles simulation using density functional theory. *Chemical Communications*, 1998(22):2455–2456, 1998.

[82] V. Bisker-Leib and M.F. Doherty. Modeling Crystal Shape of Polar Organic Materials: Applications to Amino Acids. *Crystal Growth & Design*, 3(2):221–237, 2003.

[83] Y. Kameda, H. Ebata, T. Usuki, O. Uemura, and M. Misawa. Hydration Structure of Glycine Molecules in Concentrated Aqueous Solutions. *Bulletin of the Chemical Society of Japan*, 67(12):3159–3164, 1994.

[84] K. Leung and S.B. Rempe. Ab initio molecular dynamics study of glycine intramolecular proton transfer in water. *The Journal of Chemical Physics*, 122:184506, 2005.

[85] C.E. Hughes, S. Hamad, K.D.M. Harris, C.R.A. Catlow, and P.C. Griffiths. A multi-technique approach for probing the evolution of structural properties during crystallization of organic materials from solution. *Faraday Discussions*, 136:71–89, 2007.